IS-590

IOWA STATE UNIVERSITY

PRECISE MEASUREMENT OF THE K-SHELL INTERNAL CONVERSION COEFFICIENT OF THE 344-KEV, E2 TRANSITION IN Gd^{152}

by

Guy Schupp and E. N. Hatch

AMES LABORATORY

RESEARCH AND DEVELOPMENT REPORT

U.S.A.E.C.

IS-590

Physics (UC-34)
TID-4500(24 th Ed.), October 1, 1963

UNITED STATES ATOMIC ENERGY COMMISSION
Research and Development Report

PRECISE MEASUREMENT OF THE K-SHELL INTERNAL CONVERSION COEFFICIENT OF THE 344-KEV, E2 TRANSITION IN Gd^{152}

by

Guy Schupp and E. N. Hatch

August, 1962

Ames Laboratory
at
Iowa State University of Science and Technology
F. H. Spedding, Director
Contract W-7405 eng-82

This report is distributed according to the category Physics (UC-34) as listed in TID-4500 (24th Ed.), October 1, 1963.

Legal Notice

Printed in USA. Price $ 2.25 . Available from the

Office of Technical Services
U. S. Department of Commerce
Washington 25, D. C.

TABLE OF CONTENTS

		Page
	ABSTRACT	v
I.	INTRODUCTION	1
II.	SURVEY OF THEORY	9
III.	SURVEY OF EXPERIMENTAL METHODS	18
IV.	EXPERIMENTAL INVESTIGATION	24
	A. Construction of Coincidence Spectrometer	24
	B. Measurement of the K-Shell Internal Conversion Coefficient of the 344-kev, E2 Transition in Gd^{152}	34
V.	RESULTS AND DISCUSSION	56
VI.	CONCLUSION	64
VII.	REFERENCES	65
VIII.	APPENDIX A: SOLID ANGLE MEASUREMENTS	70
IX.	APPENDIX B: ANGULAR CORRELATION FACTORS	76
X.	APPENDIX C: INTERNAL CONVERSION MEASUREMENTS IN Gd^{154} AND Dy^{160}	82
	A. Measurements in Gd^{154}	82
	B. Measurements in Dy^{160}	87

PRECISE MEASUREMENT OF THE K-SHELL INTERNAL CONVERSION COEFFICIENT OF THE 344-KEV, E2 TRANSITION IN Gd^{152} *

Guy Schupp and E. N. Hatch

ABSTRACT

A value of 0.0283 ± 0.0008 was obtained for the K-shell internal conversion coefficient, α_K, of the 344-kev, E2 transition in Gd^{152} using an electron-electron coincidence method. This value is relative to a value of 1.135 ± 0.010 for the total internal conversion coefficient, α, of the 122-kev, E2 transition in Sm^{152}. α_K/α ratios of 0.786 ± 0.004 and 0.589 ± 0.003 were measured for the 344- and 122-kev transitions, respectively. The apparent 9% discrepancy with theory for α_K of the 344-kev transition is not explained. The result is in excellent agreement with another measurement and also in agreement with an apparent lower trend for α_K's of E2 transitions in near spherical nuclei. The α_K value for the 122-kev transition is in good agreement with theory. Additional measurements were performed on the 123- and 87-kev, E2 transitions in Gd^{154} and Dy^{160}, respectively, and α_K/α ratios of 0.531 ± 0.007 and 0.341 ± 0.011 were obtained. Construction and performance of the beta-ray spectrometers used in these coincidence measurements are described along with limitations of the experimental technique.

* This report is based on a Ph. D. thesis by Guy Schupp submitted August, 1962, to Iowa State University, Ames, Iowa. This work was done under contract with the Atomic Energy Commission.

I. INTRODUCTION

One of the processes by which an excited nucleus can make a transition to a lower energy level is by internal conversion. In this process, one of the orbital electrons is ejected from the atom with an energy equal to the nuclear transition energy minus the binding energy of the electron. A usual competing process with the internal conversion mode of de-excitation is gamma-ray emission. For a given transition, the ratio of the number of internal conversion electrons ejected per second to the number of gamma rays emitted per second is the internal conversion coefficient. The measurement of these coefficients has long been a tool in nuclear spectroscopy for determining the angular momentum and parity changes in nuclear transitions. A short historical account of internal conversion investigations is given below.

The first internal conversion coefficient measurement was performed by Gurney (1) in 1925 on the RaB (Pb^{214}) and RaC (Bi^{214}) decays. He estimated, from the areas of the peaks and beta spectrum, that the probability of a RaB gamma ray being converted into a "beta ray" was 1 in 7. Homogeneous or internal conversion electrons were first observed, however, by Baeyer *et al.* (2) in 1911, and by the early twenties the energy differences between the electrons ejected from the K, L and M electronic shells by a given transition had been

explained by the Bohr model of the atom. Closely following the more refined measurements of internal conversion electrons by Ellis and Wooster (3) in 1927, Swirles (4) presented the first theory of internal conversion. She considered the nucleus to be a radiating dipole and calculated the probability of absorption in the K shell using hydrogen-like electronic wave functions in a non-relativistic formulation. These theoretical values were approximately 1/10 of the experimental values and this first discrepancy between theory and experiment was thought to be due to a neglect of the screening by the other electrons.

In 1930 studies were again made on the internal conversion lines in the electron spectrum of the RaB and RaC decays. Ellis and Aston (5) used a photoelectric method in this investigation to determine the gamma-ray intensities relative to the internal conversion electrons and obtained absolute internal conversion coefficients to an accuracy of about 30%. They pointed out the striking dependence of the coefficients on the gamma-ray energy as measured for the two nuclides. The RaB internal conversion coefficients decreased by a factor of 3 as the energy increased by only a factor of 1.5, whereas for the transitions in the RaC decay no steady variation was seen in the internal conversion coefficients as the energies varied over a factor of 3. This dependence, while qualitatively explained by Swirles' theory (4) for RaB

but not for RaC, was thought to show the effect of nuclear structure on the internal conversion process.

Casimir (6) made the first relativistic calculation for internal conversion coefficients of high energy, electric dipole transitions, and in 1932 Hulme (7) extended these calculations to energies less than the electronic mass and found agreement within 25% of experiment for three of the nine RaC transitions. In conjunction with the work of Hulme (7), Taylor and Mott (8) calculated internal conversion coefficients for electric quadrupole transitions and obtained similar agreement for the remaining RaC lines excepting the 1.42-Mev, $0^+ - 0^+$ transition. These calculations were still as much as 40% lower than the experimental values for the transitions following the RaB decay.

The next major contribution was a conceptual change in the theoretical formulation of the internal conversion process. Following their earlier work, Taylor and Mott (9) in 1933 re-examined the basic assumptions underlying the theoretical calculations and pointed out that the internal conversion process was really independent of gamma-ray emission in contrast to the concept of the gamma ray always leaving the nucleus and then sometimes interacting with an orbital electron. With this new description, the present definition of the internal conversion coefficient emerged as the meaningful quantity to consider instead of the more

intuitive ratio of internal conversion electron transition probability to the total transition probability as used previously. The two-step type process had been questioned earlier by Smekal (10) and it was not until 1953 that Bainbridge et al. (11) showed experimentally the independent nature of the internal conversion and gamma-ray processes in their study of Tc^{99m}. The theoretical activity of the early thirties in internal conversion was completed by Fisk and Taylor (12) when they calculated conversion coefficients for magnetic dipole, quadrupole and octopole transitions. The agreement between theory and experiment at this time was considered good since nearly all the experimental values could be explained by a linear combination of the appropriate electric and magnetic multipoles. These theoretical results were completely relativistic but were restricted to the K shell and to a limited energy range. The most serious restriction of the results, however, in light of later usefulness was that they were only given for Z values of 83 and 84.

With the discovery of artificial radioactivity in 1934 by Curie and Joliot (13) came the eventual need for more calculations of internal conversion coefficients. Because of the laborious nature of the calculations, various approximate methods were used before Rose et al. (14) began their systematic calculations in 1947 using the Mark I

computer at Harvard University. They extended the numerical results to a wide range of Z values and of transition energy. At the same time the extension was made to the first five electric and first five magnetic multipoles. The model for these first computer calculations was the same as had been used earlier (9,12). Following the K-shell calculations, a program was initiated by Rose to calculate internal conversion coefficients for the three L subshells. With the L-shell results a consideration of the more easily measured K/L and L-subshell ratios helped specify nuclear transitions. These L-shell calculations were first made without considering screening effects, but after the work of Reitz (15) in 1950 these effects were treated in a much more involved program which was not completed until 1956. Part of these later calculations were published in 1955 (16).

Until around 1950 and later the correctness of the theoretical results was really not questioned since the spin and parity changes of nuclear transitions were not commonly measured by other methods. As angular correlation experiments and other techniques were developed for deciphering decay schemes, the accuracy of the internal conversion coefficient calculations began to be checked experimentally. Before any significant discrepancies were found between experiment and the theoretical values of Rose et al. (14), it was pointed out by Sliv (17) that the finite size of the nucleus could

become an important factor. His subsequent calculations included nuclear surface currents as well as finite-size effects. The results of the calculations by Sliv and Band (18) using this new model showed that the K-shell internal conversion coefficients for magnetic dipole transitions in nuclei with $Z > 80$ were on the order of 40% smaller than the point-nucleus values of Rose et al. (14). The finite nuclear size calculations were substantiated by Wapstra and Nijgh (19) when they measured the internal conversion coefficient of the 279-kev transition in the decay of Hg^{203}. The method employed in this experiment was essentially the same as that used by Gurney (1) in the very first measurements of internal conversion coefficients. Many improvements in experimental techniques as well as a simple decay scheme enabled an accuracy of 3% to be obtained.

The last major development in the study of internal conversion effects came in 1956 when Church and Weneser (20) suggested that anomalous, model-dependent conversion coefficients may occur for retarded magnetic dipole transitions if one takes into account the distribution of currents throughout the nuclear volume. The term anomalous is used for these effects because they are direct consequences of the dynamical effects of nuclear structure as opposed to static effects due simply to a finite nuclear charge distribution. The electric monopole mode of nuclear de-

excitation, which finally explained the results obtained for the $0^+ - 0^+$ transition in RaC mentioned earlier, occurs only through nuclear penetration effects. A theory of the anomalous terms in the internal conversion process for electric dipole transitions was presented by Nilsson and Rasmussen (21) in 1958.

Perhaps the most logical direction for the experimental investigations of internal conversion coefficients to take would be toward finding and measuring the penetration effects. Measurements of this type have been done by Asaro et al. (22) and Gerholm et al. (23). On the other hand, since it is only by comparison with tabulated values of conversion coefficients that the additional penetration effects can be estimated, it is necessary to make comparisons between tabulated and accurately measured coefficients for transitions where penetration effects are expected to be small as was pointed out by Church and Weneser (24). The $2^+ - 0^+$, pure electric quadrupole transitions found in a large number of even-even nuclei represent such a class of transitions. The agreement between experiment and theory for this type of transition in the deformed nuclei region ($150 < A < 190$) is less than satisfactory although most of the measurements have experimental errors which are greater than 10%. With the available data, efforts have been made by Subba Rao (25) and more recently by Bernstein (26) to

correlate the apparent discrepancies between theory and experiment with the nuclear deformation.

The present investigation is concerned with accurate internal conversion coefficient measurements in the region around A = 150 where the nuclear equilibrium shape changes quite abruptly from spherical to deformed. The broader scope of this research program has included the construction of an intermediate-image beta-ray spectrometer and the modification of an existing spectrometer. The final phase of this project was to use the spectrometers together as an electron-electron coincidence spectrometer and to investigate its applicability as an instrument for accurately measuring internal conversion coefficients.

II. SURVEY OF THEORY

This survey will present the theoretical basis of internal conversion coefficient calculations. In particular, primary emphasis is given to the calculations for electric quadrupole transitions. The manner in which these calculations are made follows the framework of Rose (27) and gives an extension to the more specific surface-current-model calculations of Sliv and Band (18). From this framework, possible dynamic effects of nuclear size, discussed by Church and Weneser (24), can be estimated.

As described in the introduction, the internal conversion coefficient, α, for a nuclear transition is defined as the ratio of the number of orbital electrons ejected per second, N_e, to the number of gamma rays emitted per second, N_γ. That is,

$$\alpha = \frac{N_e}{N_\gamma} \quad . \tag{1}$$

A given transition can convert in any filled electronic shell of the atom, assuming energy conservation can be fulfilled. Thus α_K, α_{LI}, α_{LII}, α_{LIII}, etc. correspond to internal conversion coefficients for the various shells and subshells. The total internal conversion coefficient α is given by

$$\alpha = \alpha_K + \alpha_L + \alpha_M + \ldots \tag{2}$$

where $\alpha_L = \alpha_{LI} + \alpha_{LII} + \alpha_{LIII}$ and similarly for the remaining shells.

The internal conversion coefficients are strongly dependent upon the transition energy, k (in units of the electronic mass, mc^2); the atomic number, Z; the angular momentum change, L; and finally upon the parity change, $\Delta\pi$. More will be said about L and $\Delta\pi$ later but it is important to point out that it is the strong dependence of α on these two parameters which has made internal conversion measurements useful as a tool in nuclear spectroscopy.

In the following discussions, the symbols EL and ML are used for the electric 2^L and magnetic 2^L poles, respectively. In particular an electric quadrupole transition is denoted by E2 and its K-shell internal conversion coefficient by $\alpha_K(E2)$.

When the nuclear angular momenta for initial and final states are J_i and J_f, the field radiated can have any angular momentum L for which

$$\Delta J = |J_i - J_f| \leq L \leq J_i + J_f \quad . \tag{3}$$

The internal conversion coefficients are in general a mixture of the form

$$\alpha = \sum_L a(L)\alpha(L) \quad , \tag{4}$$

where a(L) represents the fraction of total gamma rays having angular momentum L; the L values are limited by Eq. 3. From the multipole expansion of the electromagnetic field, if there is no parity change in a nuclear transition there can only be emission of electric multipoles of even order (L even) or magnetic multipoles of odd order. For transitions in which there is a parity change, these even and odd orders are simply reversed.

As an example, if $J_i = 2$ and $J_f = 1$ and there were no parity change, the radiated field would be a mixture of M1, E2 and M3. From Eq. 4, the K-shell internal conversion coefficient for this transition would be

$$\alpha_K = a(1)\alpha_K(M1) + a(2)\alpha_K(E2) + a(3)\alpha_K(M3) \quad , \qquad (5)$$

where $a(1) + a(2) + a(3) = 1$. For mixtures of this type, the $a(1)/a(3)$ ratio is usually so large that the M3 component can be neglected. Similarly,

$$\alpha_L = a(1)\alpha_L(M1) + a(2)\alpha_L(E2) \text{ and } a(1) + a(2) = 1 \qquad (6)$$

where the L subscript refers to the electronic shell as in Eq. 2.

The mixing ratio, $\delta = \frac{a(2)}{a(1)}$, can be determined from the theoretical values of the internal conversion coefficients and the experimentally measured α_K/α_L (or simply K/L) ratio according to the relation

$$\delta = -\frac{\alpha_K(M1) - (K/L)\alpha_L(M1)}{\alpha_K(E2) - (K/L)\alpha_L(E2)} \quad . \tag{7}$$

Conversely, if δ can be determined from some other independent measurement (angular correlation for example), a check can be made on the accuracy of the internal conversion coefficient calculations. Of importance to the present investigation is the fact that when $J_i = 2$ and $J_f = 0$ and there is no parity change, the only possible multipole is E2. For these pure E2 transitions there are no uncertainties or errors introduced in the measurements from a determination of mixing ratios.

Two basic assumptions are made in formulating the theory of internal conversion. The first is the use of perturbation theory in calculating transition probabilities. By virtue of their charge and motion, the nucleus and orbital electrons are coupled via the electromagnetic field and may therefore exchange virtual quanta resulting in the transition: Nucleus in excited state + bound electron $\longrightarrow$ nucleus in lower state + electron in continuum. Second-order perturbation theory is needed for the calculation of N_e while only first-order theory is needed for the calculation of N_γ wherein the nucleus emits real quanta. The second assumption consists of the statement that the electron is described by a Dirac one-particle theory. When screening is taken into account, the nuclear potential is modified but it is still of a central character.

With the above assumptions, the appropriate transition rates as given by Rose (27) are:

$$N_\gamma = 8\pi\alpha k \mathcal{S}_N \left| \int d\tau_N \vec{J}_N \cdot \vec{A}^*_{LM} \right|^2 \tag{8}$$

$$N_e = 2\pi\alpha^2 \mathcal{S}_e \left| \int d\tau_N \int d\tau_e (\vec{J}_N \cdot \vec{J}_e - \rho_N \rho_e) \frac{e^{ik|\vec{r}_N - \vec{r}_e|}}{|\vec{r}_N - \vec{r}_e|} \right|^2 . \tag{9}$$

In Eqs. 8 and 9, α is the fine structure constant. $\mathcal{S}_N$ is a sum over final and average over initial nuclear substates. $\mathcal{S}_e$ contains in addition to these operations, a sum over final electron states and a sum over magnetic quantum numbers of the initial state. $\vec{J}_N$ and $\vec{J}_e$ are transition current densities for the nucleon and electron, respectively; ρ_N and ρ_e are transition charge densities. These densities are assumed to obey the usual continuity equations,

$$\text{div } \vec{J}_N = ik\rho_N \quad \text{and} \quad \text{div } \vec{J}_e = -ik\rho_e \quad . \tag{10}$$

$\vec{J}_e$ and ρ_e are defined in terms of the Dirac matrices and the Dirac one-electron wave functions of the initial and final states. With few restrictions, the internal conversion coefficient calculations based only on the static effect of nuclear size are insensitive to the specific forms chosen for $\vec{J}_N$ and ρ_N. $\vec{A}_{LM}$ is the vector potential of the appropriate 2^L pole where M is the magnetic quantum number change in the

nuclear transition.

Expansion of the expression for N_e in Eq. 9 is given elsewhere (24,28), but it is important to consider at least qualitatively the results obtained for this expansion and their dependence on whether or not the electron is restricted to a region outside the nuclear radius. In the earlier point-nucleus calculations of Rose et al. (14), the expansion for N_e gave nuclear matrix elements identical to those in N_γ, and the resulting internal conversion coefficients were independent of nuclear structure. If the nucleus is considered to have finite dimensions, however, the small-distance behavior of the electron wave functions is modified, and in addition the expansion of N_e gives some matrix elements which are different from those in N_γ. The nuclear matrix elements then fail to cancel and give rise to what are called penetration terms in the calculations of the internal conversion coefficients; these terms would vanish if the electron current density were zero inside the nucleus. Since a knowledge of $\vec{J}_N$ or the nuclear wave functions is needed to calculate these terms, they are subject to the particular nuclear model chosen and are referred to as the dynamic effects of nuclear size.

The dynamic effects are usually small but can become important in cases where the gamma-ray matrix element is anomalously small. While not of primary concern in this

investigation, these effects are considered in more detail in the discussion of the results.

For K shell internal conversion of E2 transitions, the ratio of Eq. 9 to Eq. 8 reduces to

$$\alpha_K(E2) = \frac{\pi\alpha k}{30}\sum_{\varkappa} C_{\varkappa,-1}|R_\varkappa + \Delta R_\varkappa|^2 \quad , \tag{11}$$

where $\varkappa$ takes on the two values, 2 and -3, for which the numerical coefficient $C_{\varkappa,-1}$ is 4 and 6, respectively. The parameter $\varkappa$ is a non-zero integer which specifies the total angular momentum quantum number $j = |\varkappa| - 1/2$ and the parity quantum number $\ell = j + \frac{\varkappa}{2|\varkappa|}$ for the final electron state. With this same convention, the -1 subscript corresponds to the $s\frac{1}{2}$ electron bound in the K shell. The radial integrals representing all static effects are given by

$$\begin{aligned} R_\varkappa = {} & (-1-\varkappa)\int_0^\infty h_1(g_\varkappa f_{-1} + f_\varkappa g_{-1})r^2dr \\ & + 2\int_0^\infty\left[h_1(g_\varkappa f_{-1} - f_\varkappa g_{-1}) + h_2(f_\varkappa f_{-1} + g_\varkappa g_{-1})\right]r^2dr \quad , \end{aligned} \tag{12}$$

where h_1 and h_2 are spherical Hankel functions of the first kind with argument kr; $f_\varkappa$ and $g_\varkappa$ are radial functions for the final state; f_{-1} and g_{-1} are radial functions for the initial state.

The primary problem of the calculations is the computation of the radial integrals of Eq. 12. For this

purpose it is necessary to carry out numerical solutions of the radial wave equations

$$\frac{d}{dr}\begin{pmatrix} f \\ g \end{pmatrix} = \begin{pmatrix} \frac{\varkappa - 1}{r} & -(W-1-V) \\ W+1-V & -\frac{(\varkappa+1)}{r} \end{pmatrix}\begin{pmatrix} f \\ g \end{pmatrix}, \qquad (13)$$

where the units are such that $mc^2 = 1$ and $\hbar/mc = 1$. For the bound states, the central potential V is taken to be that of a uniform charge distribution inside the nuclear radius and a Thomas-Fermi-Dirac screened potential outside the nuclear radius. W is the energy of the electron state. A nuclear radius of $1.2\ A^{1/3}\times10^{-13}$ cm was used in the calculations by Rose (27) and a 10% change in R generally leads to changes in the coefficients of less than 1%.

The factors in Eq. 11 which allow for possible dynamic effects of nuclear size are

$$\Delta R_{-3} = -R_{-3}\omega_{-3}\, e^{i\tau_{-3}}\left[E_2^{(1)} + E_2^{(2)}\right] \qquad (14)$$

and

$$\Delta R_2 = -R_2\omega_2\, e^{i\tau_2}\left[\frac{\overline{b_o}}{U_2} E_2^{(1)} + \frac{\overline{c_o}}{U_2} E_2^{(2)}\right], \qquad (15)$$

where $E_2^{(1)}$ and $E_2^{(2)}$ depend on the nuclear model chosen and for the surface-current-model calculations (18) are

1 and $\sqrt{2/3}$, respectively. These terms are set equal to zero in the static, finite-size calculations of Rose (27). The remaining parameters are defined and tabulated as functions of Z, k and L by Green and Rose (28,29). Magnitudes for these parameters as they apply to this experimental investigation are given in the discussion of the results.

III. SURVEY OF EXPERIMENTAL METHODS

There are many different methods for measuring internal conversion coefficients but the majority of them have experimental errors of $\geq$ 10%. In this section, the main emphasis will be given to only the most accurate techniques and their applications to pure E2 transitions.

Since the internal conversion coefficient is simply the ratio of electrons ejected to gamma rays emitted for a nuclear transition, any experimental method must utilize the detection of at least one of these forms of radiation. In experimentally determining these quantities, the gamma-ray spectrum is usually complicated by many gamma-ray peaks and the electron spectrum usually has beta particles as well as internal conversion electrons from several transitions. Thallium activated sodium iodide crystals, NaI(Tl), connected to photomultiplier tubes with the associated electronics, make up the conventional gamma-ray scintillation spectrometers. Variable magnetic field spectrometers are commonly used for measuring the electron spectra and will be discussed more fully in the next section. Although bent-crystal gamma-ray spectrometers and fixed field electron spectrographs are used primarily for accurate energy determinations, they can sometimes give precise ratios for internal conversion coefficients of several transitions occuring in a particular

decay scheme.

For very simple decay schemes, careful measurements of either the electron or gamma-ray spectrum can give accurate internal conversion coefficients. The measurement of Wapstra and Nijgh (19) on Hg^{203} mentioned earlier was of this type. They measured the electron spectrum and resolved it into the internal conversion electron and beta-ray components. The ratio of the number of K-shell internal conversion electrons to the number of beta rays minus the total number of internal conversion electrons gave α_K for the 279-kev transition to an accuracy of 3%.

Measurements on simple gamma-ray spectra by McGowan and Stelson (30) in 1957 were the first to point out possible discrepancies between experiment and theory for pure E2 transitions. Since K shell internal conversion leaves a hole in that electronic shell, the internal conversion process will be subsequently followed by a K x ray (with a probability equal to the fluorescent yield). These x rays along with the gamma rays were detected with a NaI(Tl) crystal. The ratio of the number of K x rays to the number of gamma rays, both properly normalized, gave α_K's with errors from 20% down to 7% at best.

Another way to measure internal conversion coefficients accurately is the internal-external method of Hultberg and Stockendal (31) which is a careful extension of

the photoelectric method of Ellis and Aston (5). In experiments of this type, a magnetic beta-ray spectrometer is used to measure the internal conversion electrons from a transition of interest and then to measure the number of electrons ejected from an external converter, placed near the source, by the corresponding gamma ray. The number of external electrons is proportional to the product of the number of gamma rays and the photoelectric cross-section of the converter. The energy dependence and absolute values of the photoelectric cross-sections can be calculated but must usually be normalized by comparison with some accurately known internal conversion coefficients. Once this is done, however, the ratio of the internal conversion electrons to the externally converted electrons can be multiplied by the photoelectric cross-section to give the internal conversion coefficient. Limitations of this method are an intense yet thin source and an accurate knowledge of the converter thickness and uniformity, but its wide range of applicability and good accuracy make it quite useful. The recent work of Frey et al. (32) demonstrates this statement and gives a minimum error of 2.1% with 5% being more typical.

The remainder of the most accurate methods for measuring internal conversion coefficients utilizes coincidence techniques. The simple coincidence logic requires some specified electron or gamma-ray event to occur simulta-

neously (within 10^{-8} sec) with the transition of interest. The only accurate method for measuring internal conversion coefficients with only gamma-ray scintillation spectrometers for detectors is the coincidence-sum method of Lu and Schupp (33). This method is an extension of the summing method due to Lu (34) which was severely limited in its applicability. The essential feature of the method is the requirement of a high energy gamma ray to be followed in coincidence by only a low energy transition whose gamma ray must be completely absorbed in the summing crystal. In this way the total internal conversion coefficient for the low energy transition can be deduced. Although the coincidence and energy requirements restrict this method, it is the most accurate one for measuring total internal conversion coefficients of some of the low energy, E2 transitions in the deformed nuclei. Accuracies of approximately 1% can be obtained for the total internal conversion coefficients resulting in errors of 1% or greater for the K-shell coefficients when these measurements are combined with internal conversion ratios measured with a beta-ray spectrometer.

Recently, Taylor and Merritt (35) measured the total internal conversion coefficient of the 166-kev transition in the very simple electron capture of Ce^{139} to an accuracy of 0.5%. Coincidences were taken between the 166-kev gamma ray and a 4π proportional counter whose sensitivity to Auger

electrons, x rays and internal conversion electrons was varied by a series of thin absorbers. The details of this method have not been published but it is expected to be quite inflexible in its applicability.

The other possibilities for the coincidence technique involve electron-electron and electron-gamma ray coincidence measurements and have been described in detail by Gerholm (36). For accurate determinations of conversion coefficients, this method requires that a resolved gamma ray or electron (from either internal conversion or a beta-ray group) must be in coincidence with the transition whose internal conversion coefficient is to be measured. The number of coincidences for a particular transition depends upon the transmission of the lens spectrometer, the α_K/α internal conversion ratio and the internal conversion coefficient. The spectrometer transmission is a principal source of error in these measurements but with care it can be determined absolutely to an accuracy of $\geq$ 2%. In other cases, internal conversion coefficients measured accurately by other methods can be used to determine the transmission of the spectrometer. Wherever applicable, coincidence measurements of this type are the most straightforward method for determining internal conversion coefficients to an accuracy of approximately 3%.

Use of the electron-electron coincidence method

comprises the main body of this investigation and is discussed further in the following section.

IV. EXPERIMENTAL INVESTIGATION

The first part of this section is concerned with the actual construction and performance of the coincidence spectrometer, and the second part describes the particular experiments performed.

A. Construction of Coincidence Spectrometer

The idea of studying electron-electron coincidences was first forwarded by Feather (37) in 1940 and was subsequently implemented by him in collaboration with Kyles and Pringle (38) in 1948. For these first measurements a permanent magnet spectrograph with movable Geiger counter detectors was used. Since that time, gradual improvement of coincidence spectrometers with greater collecting power or transmission has been made. In 1951 Siegbahn (39) constructed a so-called "spectrogoniometer" which consisted of two thin lens spectrometers whose axes could be oriented between 180° and 90°. The transmission and resolution of the spectrometers were 0.3% and 2.2%, respectively, when a 3 mm diameter source was used. Further progress toward higher transmission was made by Gerholm (40). He internally divided a long lens, iron shielded spectrometer and obtained a transmission of 3% with a resolution of 1.3% in each half of the spectrometer

using a 2 mm source. At the same transmission, a source diameter of 5 mm gave a resolution of 3.1%.

Since the number of coincidence counts increases by a factor f^2 if the transmission in each channel of the coincidence spectrometer is increased by a factor f, the possibility of utilizing the high transmission characteristics of the Slätis-Siegbahn type intermediate-image spectrometer (41) was first investigated by Slätis and Herrlander (42) in 1955. A recent article (43) by them describes in detail the construction and performance of their coincidence spectrometer. Its typical transmission and resolution values are given later in comparison with the present work.

Another important feature regarding instruments of the lens type is their size. Although they could in principle be made quite small, the source diameter would also have to be scaled down to preserve the same transmission and resolution characteristics. For a specified thickness, the source intensity depends on the source area, and it is therefore desirable for most cases to make the physical dimensions of a spectrometer as large as is conveniently possible. A Slätis-Siegbahn type intermediate-image spectrometer whose pertinent dimensions were a factor of 1.2 larger than those used by Herrlander and Slätis was constructed by Nichols et al. (44,45) in 1953 at Iowa State University. The schematic cross-section of the spectrometer constructed by Nichols et

al. is shown in Fig. 1.

The present investigation began in 1956 when plans were made to build another spectrometer of the same size which could be used in coincidence with the existing spectrometer after some modifications. Except for the necessary modification of the magnetic yoke to allow for the source and detector positions to be outside the yoke, differences in construction between the new and existing spectrometer were limited to minor changes in the cooling and baffle systems. A schematic cross-section of the coincidence spectrometer is shown in Fig. 2. The machine work for the spectrometers was performed in the Iowa State University Instrument Shop. Details of winding the coils on the brass spool were carried out in a manner almost identical with the procedure described by Nichols et al. (44); the only difference being that each coil instead of pairs of coils was externally connected to the water system to provide more efficient cooling. The brass spacer shown between the spectrometers in Fig. 2 also determines the source position and can be fastened to either spectrometer and moved along two perpendicular directions by means of screw adjustments to position the source on the magnetic axes.

Although most of the existing systems including current and safety controls carried over into the present construction, some engineering details unique to the coinci-

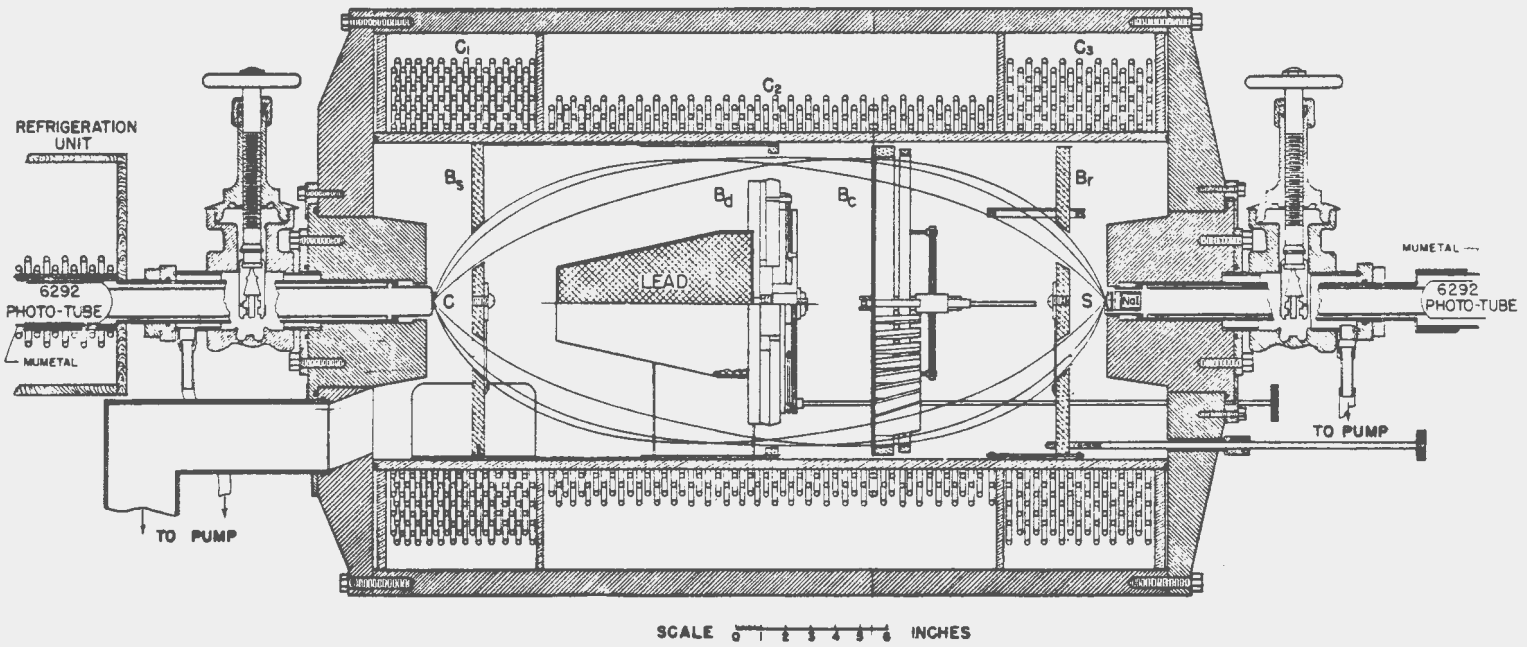

Fig. 1. Schematic cross-section of intermediate-image beta-ray spectrometer.

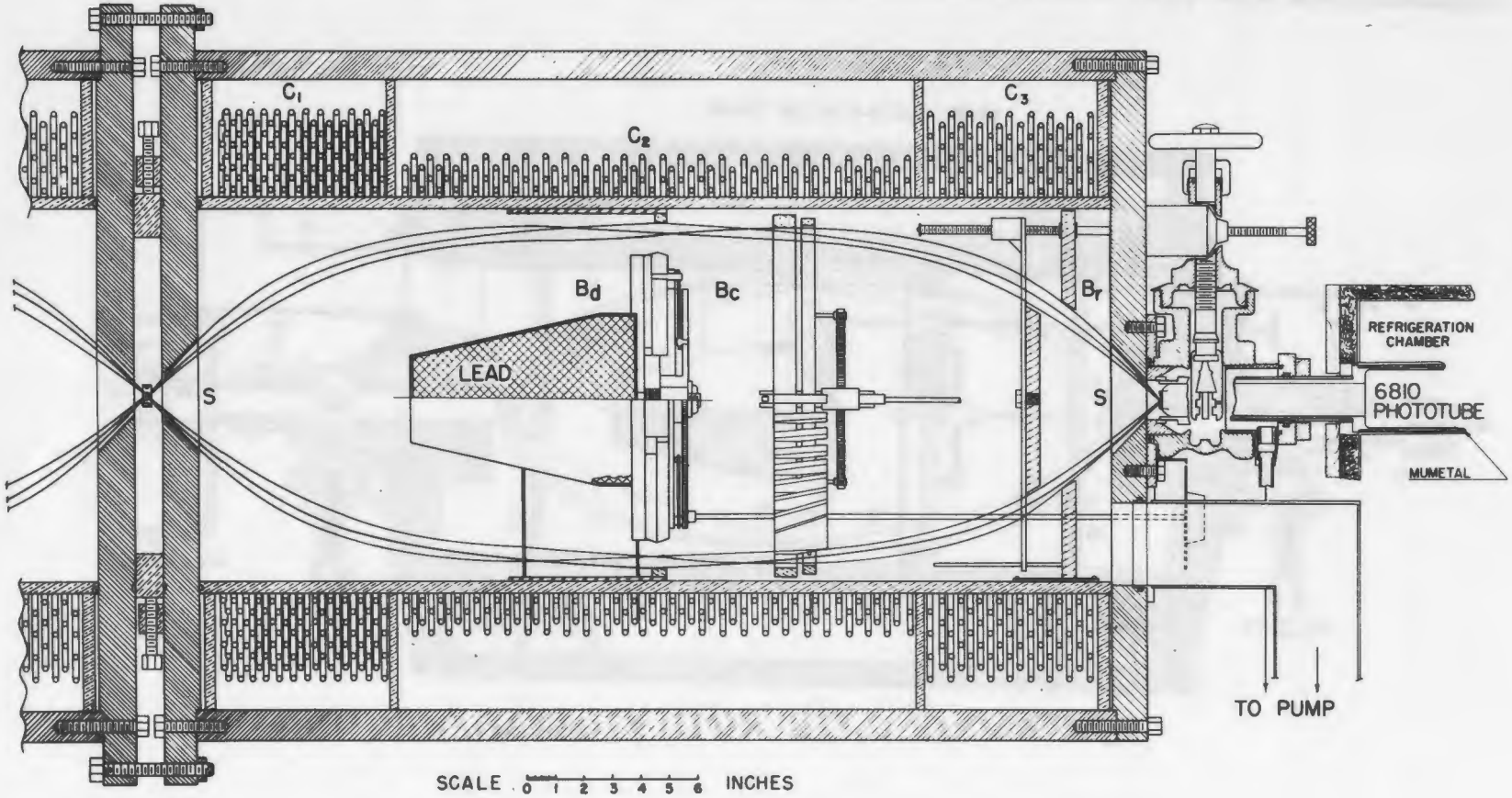

Fig. 2. Schematic cross-section of electron-electron coincidence spectrometer.

dence arrangement were involved. These included a movable table which would support the approximate one ton weight of the new spectrometer, a flexible water system capable of holding the 300 psi input pressure to the coils, and provisions for aligning the axes of the two spectrometers. A careful study of the photograph shown in Fig. 3 reveals the way in which these new demands were met.

Following completion of the new spectrometer, checks were first made on the symmetry of the magnetic field. With neither end plate mounted and with all the coils connected in series, the measured magnetic field intensity along the axis is shown in the lower curve of Fig. 4. Also shown is a similar measurement made with only one of the end plates in position. These curves were taken with a current of 4 amps through the coils. A General Electric Gaussmeter and a Rawson fluxmeter were used to measure the field intensity inside and outside of the iron yoke, respectively. As seen from Fig. 4, the magnetic field at the source position is a factor of 30 lower than the maximum field strength, and little or no influence of one spectrometer on the other was expected. A later check on this possible effect showed that the momentum displacement of the 60-kev Auger lines in Pb^{207} was less than 0.1% when the field in the other spectrometer was changed from zero up to a value corresponding to an electron energy of about 3 Mev (60 amps). The optimum field shape

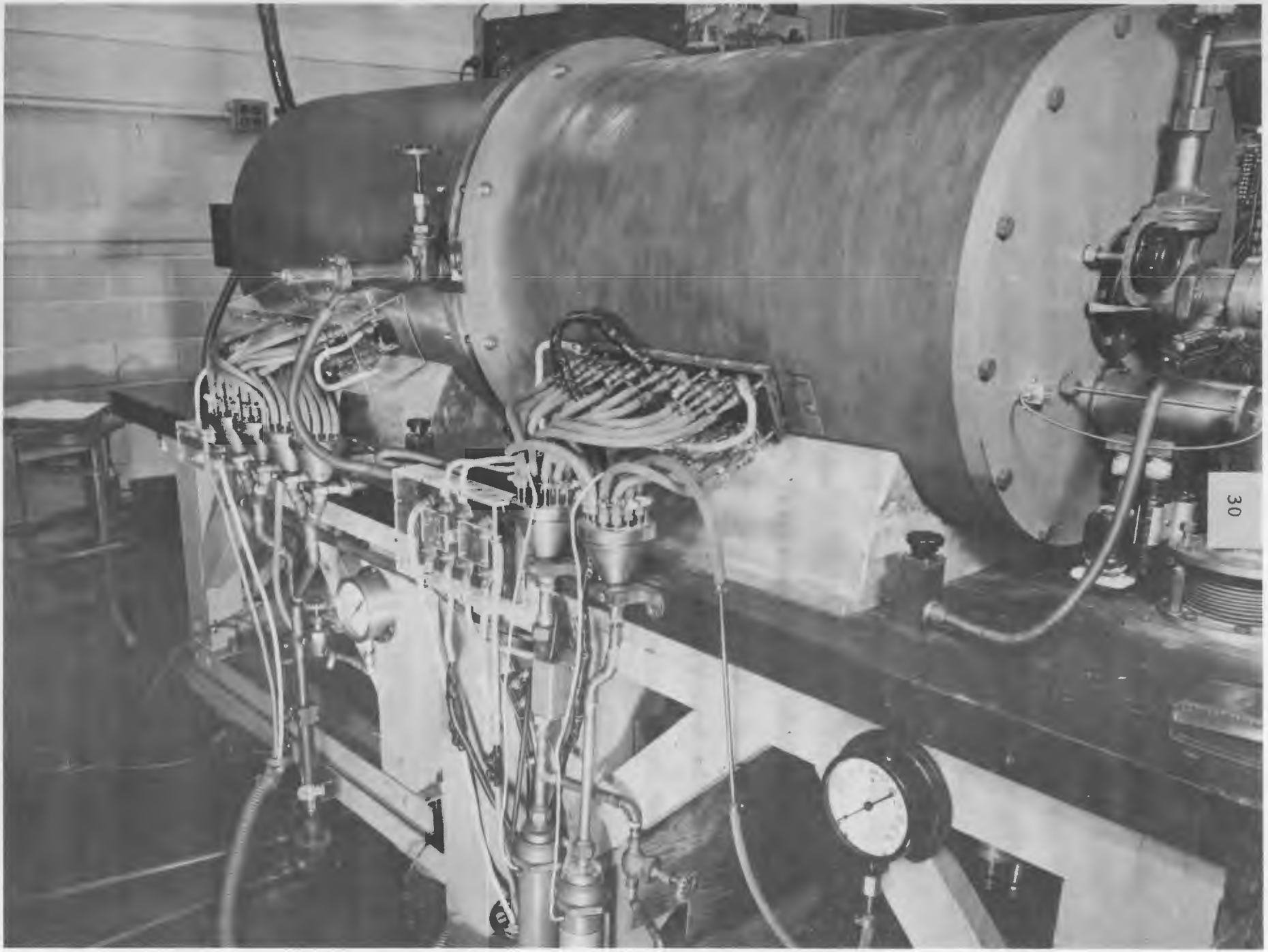

Fig. 3. Photograph of spectrometers arranged for electron-electron coincidence measurements.

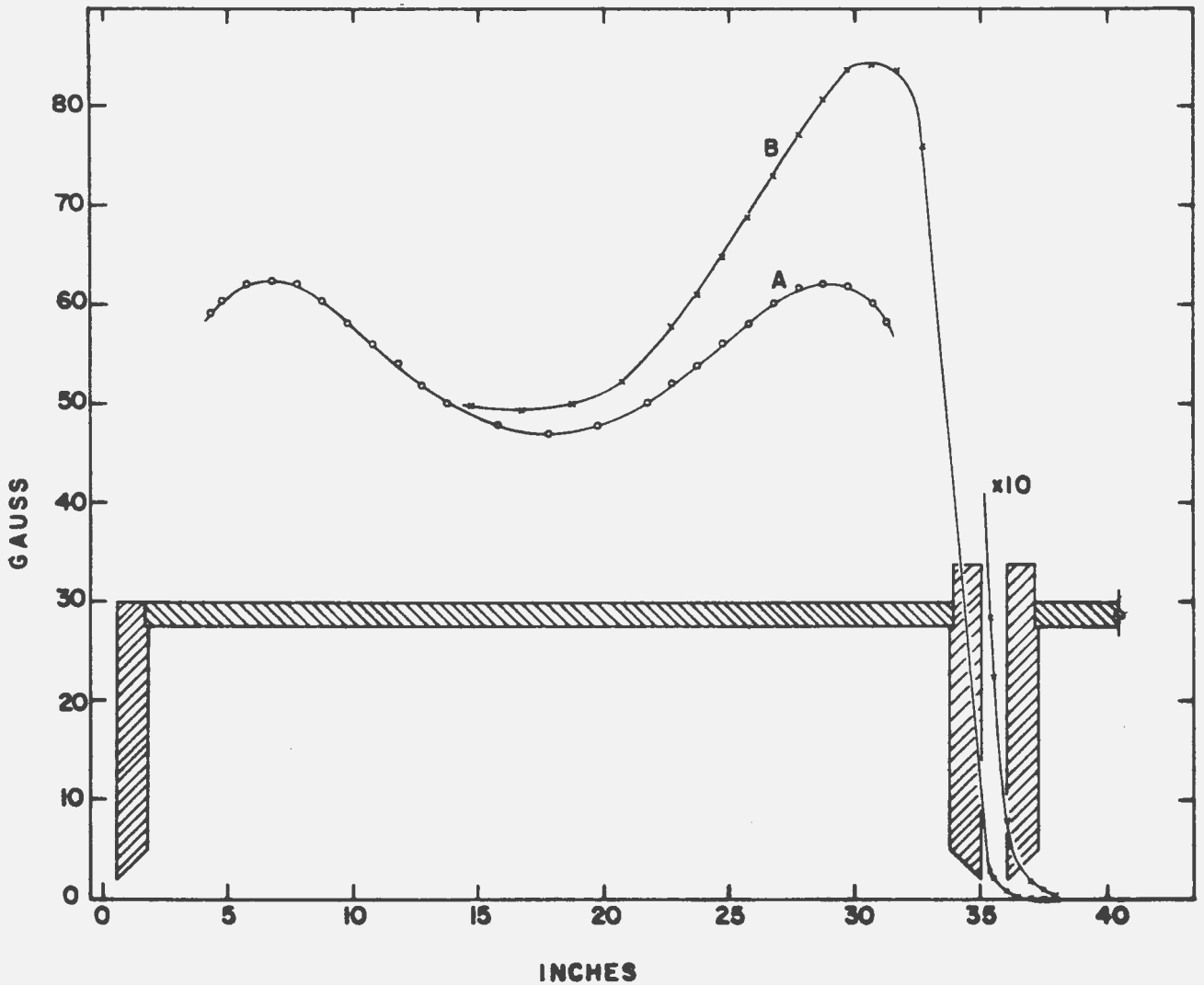

Fig. 4. Axial magnetic field distribution in spectrometer.

A. Without end plates.
B. With one end plate in position.

determined by maximum transmission was obtained by electrically omitting 3 of the 4 center coils as well as 3 of the 10 coils in each of the two end sections.

Using different source sizes, a series of relative transmission versus resolution curves were deduced from data taken by scanning over the ThB F-line with different center and resolving baffle settings. The relative transmission values were experimentally found to be in agreement with the expression

$$T_{rel} = T_o \left[1 - f \, (a^2/2 + h^2) \right] \quad , \qquad (16)$$

where T_o is the transmission for a point source on the axis, a is the source radius and h is the distance between the center of the source and the spectrometer axis. The coefficient f has the values 0.035 ± 0.004 mm^{-2} and 0.068 ± 0.007 mm^{-2} for transmission based on peak areas and peak heights, respectively. The combination of these results with the absolute value for the peak height transmission discussed in Appendix A gives the curves shown in Fig. 5. Table I lists typical transmission and resolution values and compares them with the corresponding values obtained by Herrlander and Slätis (43).

The performance of the spectrometers as independent instruments has been reported by Nichols et al. (46) for the new spectrometer used in beta shape factor investigations and

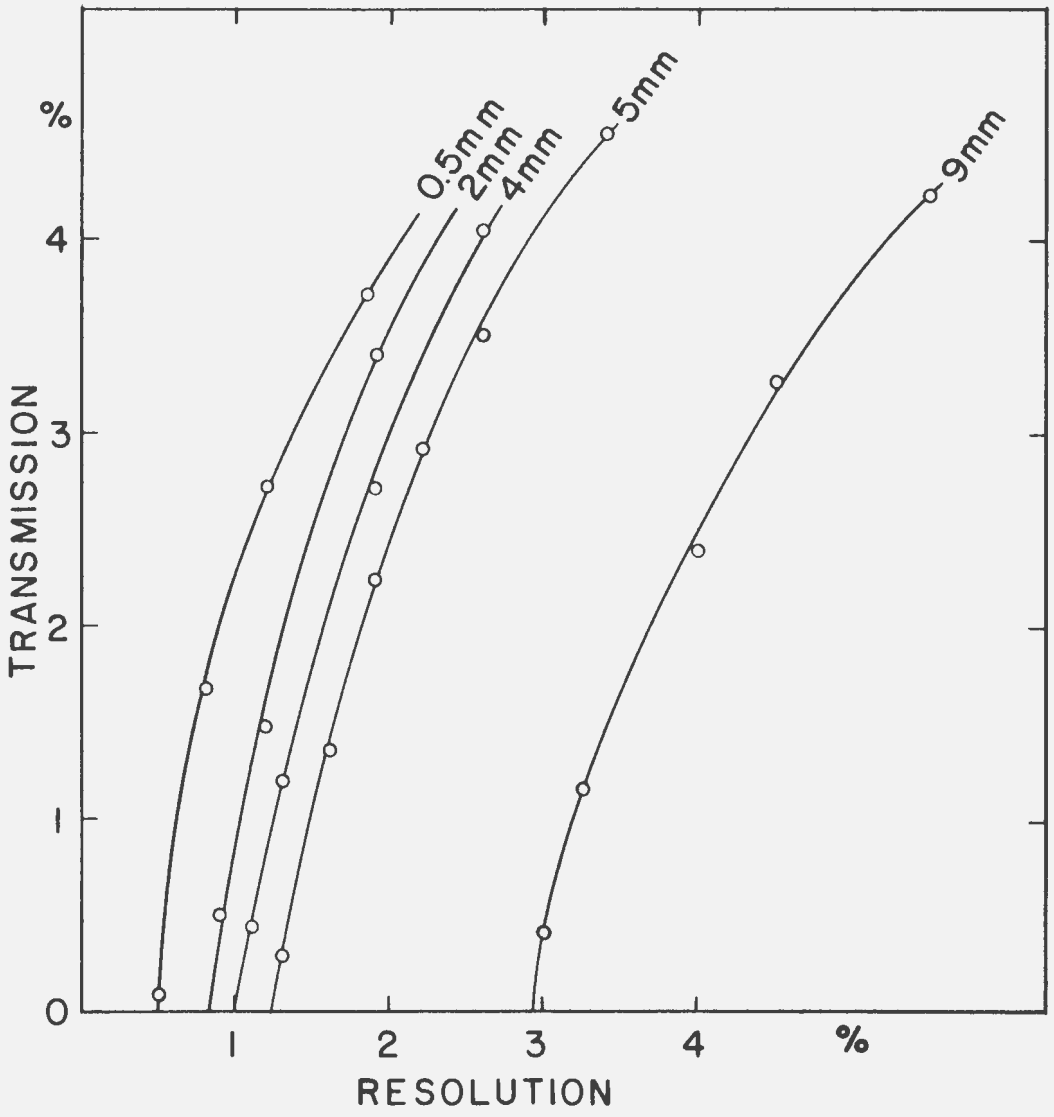

Fig. 5. Transmission versus resolution characteristics for different source sizes in the new or modified spectrometer.

Table I. Transmission and resolution values taken from Fig. 5

	Source diameter, mm									
	9		5		4		2		1/2 (1)	
T[a], %	4	2	4	2	4	2	4	2	4	2
R[b], %	5.2	3.7	3.0	1.8	2.6	1.6	2.3	1.4	2.1	0.9
R[c], %					2.7	1.9	2.0	1.2	(1.9)	(0.9)

[a]Transmission values.

[b]Resolution values.

[c]Comparable resolution values obtained by Herrlander and Slätis (43).

by Schupp et al. (47) for the modified spectrometer used in beta-gamma coincidence studies. The present investigation was the first to use the spectrometers in the coincidence arrangement and has primarily examined its applicability to accurate internal conversion coefficient measurements.

B. Measurement of the K-Shell Internal Conversion Coefficient of the 344-kev, E2 Transition in Gd^{152}

The sample used in this investigation was produced by slow neutron irradiation of enriched (97.8%) $Eu_2^{151}O_3$ in a reactor at the Oak Ridge National Laboratory. Eu^{152} was chosen because it decays by electron capture to Sm^{152} as well

as by beta emission to Gd^{152}. The decay scheme (48,49) is given in Fig. 6. It has been well established that the equilibrium nuclear shape changes rapidly, in the nature of a "jump", in the region of neutron number N = 88 to N = 90 (50,51). Gd^{154}, with N = 90 and Z = 64, is known to have an ellipsoidal shape and exhibits rotational type low lying levels as can be seen from the decay scheme (49) shown in Fig. 7. Sm^{152}, also with N = 90 but Z = 62, is very similar in shape and level structure, as well as in other collective properties. Gd^{152}, on the other hand, with N = 88 and Z = 64, has a near-spherical shape and exhibits vibrational type low lying levels quite different from that of Gd^{154}. Accurate measurements of internal conversion coefficients in this region would therefore be expected to give information relevant to the possible correlations between nuclear deformation and internal conversion suggested by Subba Rao (25) and Bernstein (26).

Independent determinations of α_K for the pure E2, 122- and 344-kev transitions in Sm^{152} and Gd^{152} could be made using the electron-electron coincidence method if the solid angle of one of the spectrometers were accurately known. A Hg^{197m} source was used for a solid angle measurement but the results were imprecise and are discussed in Appendix A. Another attempt to measure the solid angle was not tried since α_K of the 344-kev transition could be deter-

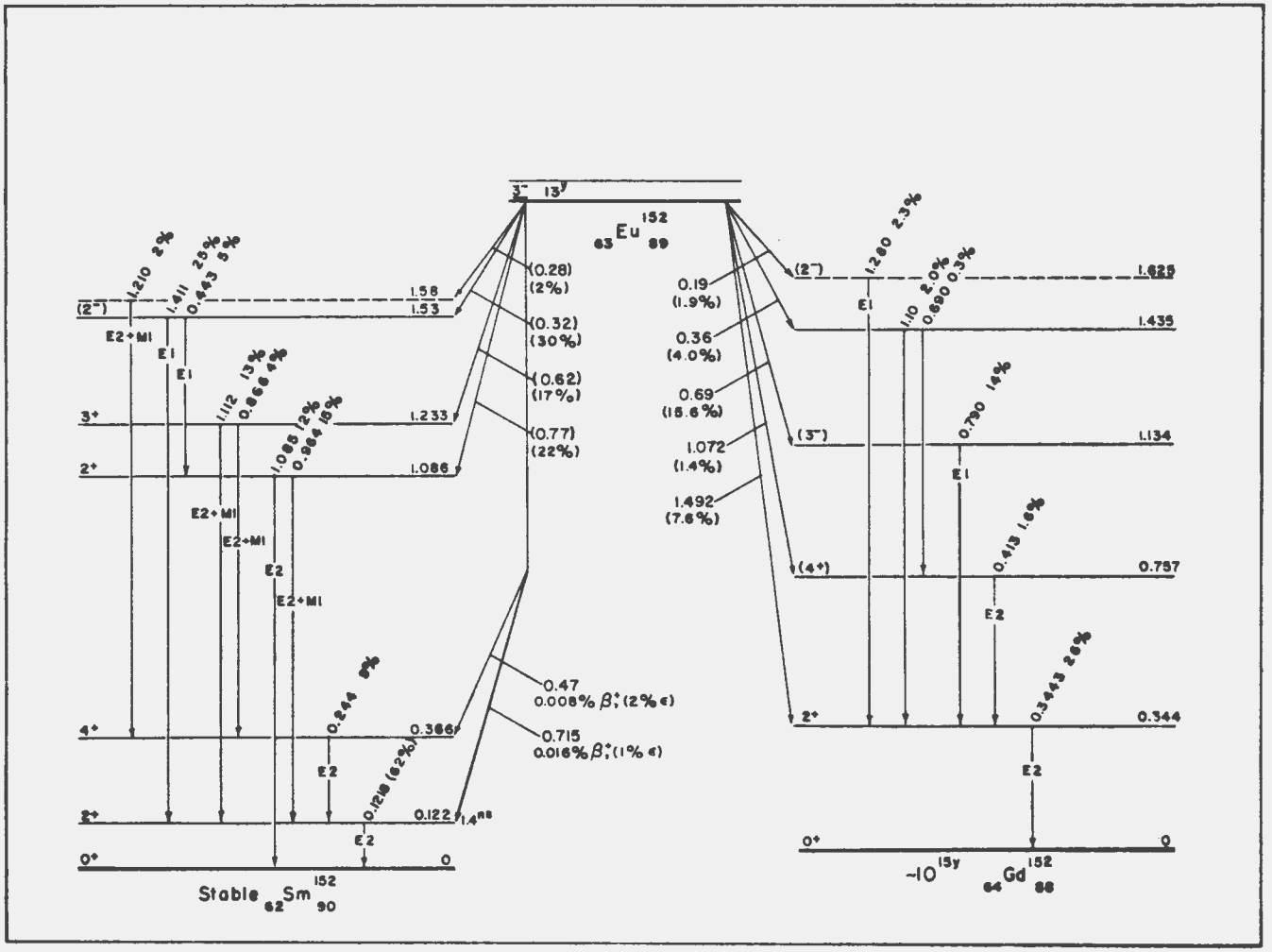

Fig. 6. Decay scheme of Eu^{152} (energies in Mev).

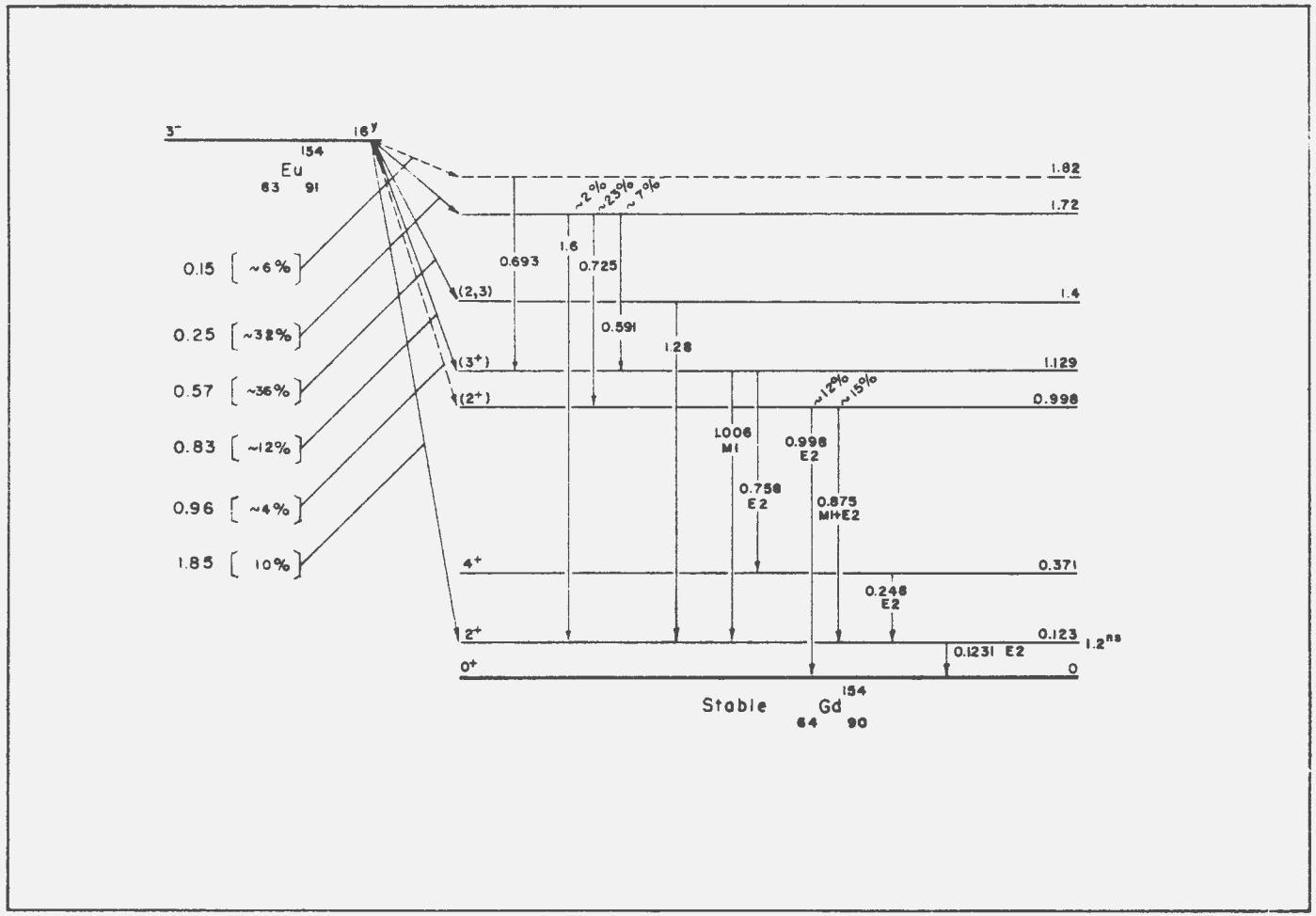

Fig. 7. Decay scheme of Eu^{154}.

mined relative to α_K of the 122-kev transition quite accurately, and the total internal conversion coefficient of the latter transition has been measured by Lu and Schupp (52) to be 1.135 ± 0.010.

A $EuCl_3$ source was used in the first relative measurement and a EuF_3 source was used in a later experiment. These sources were vacuum evaporated from the dilute HCl and HF solutions of the enriched Eu^{152} activity described above. The source films were aluminized formvar with a total thickness of 18 ± 4 $\mu g/cm^2$. Orifices 5 mm in diameter were used to define the source areas and to center them on the films. Source thicknesses were estimated to be less than 1 $\mu g/cm^2$.

Considering first the measurement on the 344-kev transition in Gd^{152} and referring to the block diagram shown in Fig. 8 as well as to the decay scheme, if Spec. 1 is set at an electron energy of 480 ± 25 kev, then each of the beta particles detected would be in coincidence with an ensuing 344-kev transition. With Spec. 2 set on the peak of the 344 K-internal conversion line, the number of coincidence counts, $N_c(344)$, would be given by

$$N_c(344) = N_1(\beta)\,[\,1+\alpha(344)\,]^{-1}\,\alpha_K(344)\,\Omega_2\,\epsilon_2(344)\cdot \epsilon(\text{coin})\,C(\beta\text{-}344)\,, \tag{17}$$

where $N_1(\beta)$ is the number of beta counts detected by Spec. 1,

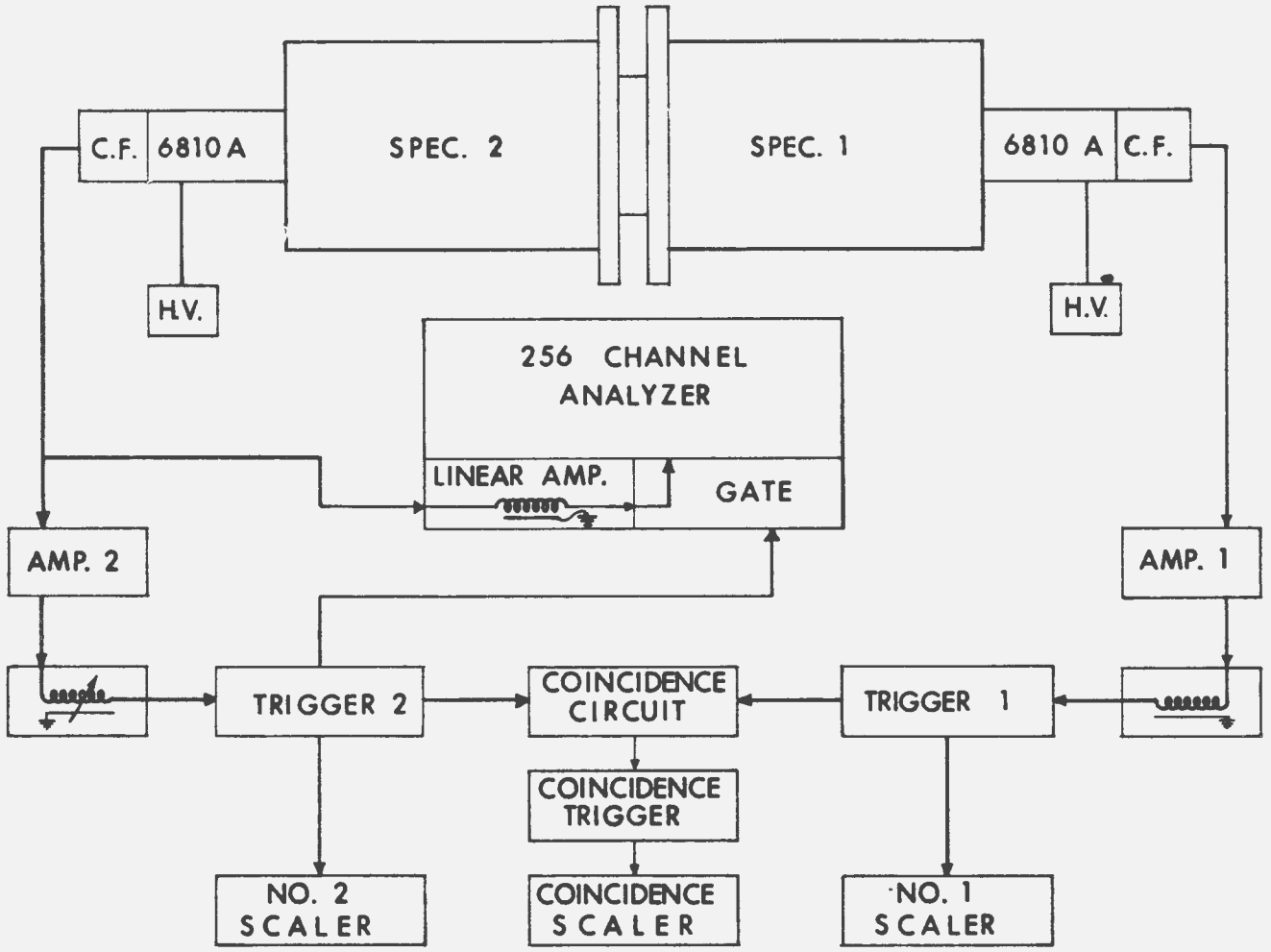

Fig. 8. Block diagram of equipment used in this investigation.

$\alpha(344)$ and $\alpha_K(344)$ are the total and K-shell internal conversion coefficients of the 344-kev transition, Ω_2 is the solid angle of Spec. 2, $\epsilon_2(344)$ is the detection efficiency of Spec. 2 for the 344 K-internal conversion electrons, ϵ(coin) is the efficiency of the coincidence circuit, and C(β-344) is the factor which arises from angular correlation effects between the betas and the internal conversion electrons.

Consider now the 122-kev measurement, realizing that nothing has been changed regarding the source. If Spec. 1 is set on the K-internal conversion line of the 245-kev transition in Sm^{152}, and Spec. 2 is set on the peak of the 122 K-internal conversion line, the number of coincidence counts would be

$$N_c(122) = N_1(245K)\,[1+\alpha(122)]^{-1}\,\alpha_K(122)\,\Omega_2\,\epsilon_2(122)\cdot \epsilon(\text{coin})\,C(245\text{-}122)\,, \tag{18}$$

where the notation is analogous to that above with the 1 and 2 subscripts designating the spectrometers, and the numbers in parentheses refer to the particular transitions.

If the ratio of Eqs. 17 and 18 is taken, the following expression is obtained

$$\frac{N_c(344)/N_1(\beta)}{N_c(122)/N_1(245K)} = \frac{[1+\alpha(122)]}{[1+\alpha(344)]} \frac{\alpha_K(344)}{\alpha_K(122)} \frac{\epsilon_2(344)}{\epsilon_2(122)} \frac{C(\beta-344)}{C(245-122)}, \quad (19)$$

where the ϵ(coin) and Ω_2 quantities have been eliminated.

It is assumed that the coincidence efficiency factors in Eqs. 17 and 18 are the same. Since 2τ 's of approximately 0.35 μsec were used in this investigation, ϵ(coin) is expected to be close to unity. Prompt coincidence curves of the type shown in Fig. 9 were always measured before any particular coincidence data were taken. The delay was then set, as indicated by the arrow at the center of the prompt distribution in Fig. 9, such that transit time or energy dependent effects would be minimized. Any error contribution to Eq. 19 from the ratio of the ϵ(coin)'s for the two measurements is then expected to be less than 0.5%. Although the resolving times used were rather long, the accidental coincidences never amounted to more than 5% of the total coincidences across the peaks because of the low counting rates. The accidentals were calculated from the 2τ values measured by feeding pulses from a pulse generator through the circuits associated with Spec. 1 before and after each coincidence run. These values were also in good agreement with the full width at half maximum of the corresponding prompt curves.

It is also assumed that Ω_2 is the same for the 122 and 344 K-internal conversion electrons. If the electron

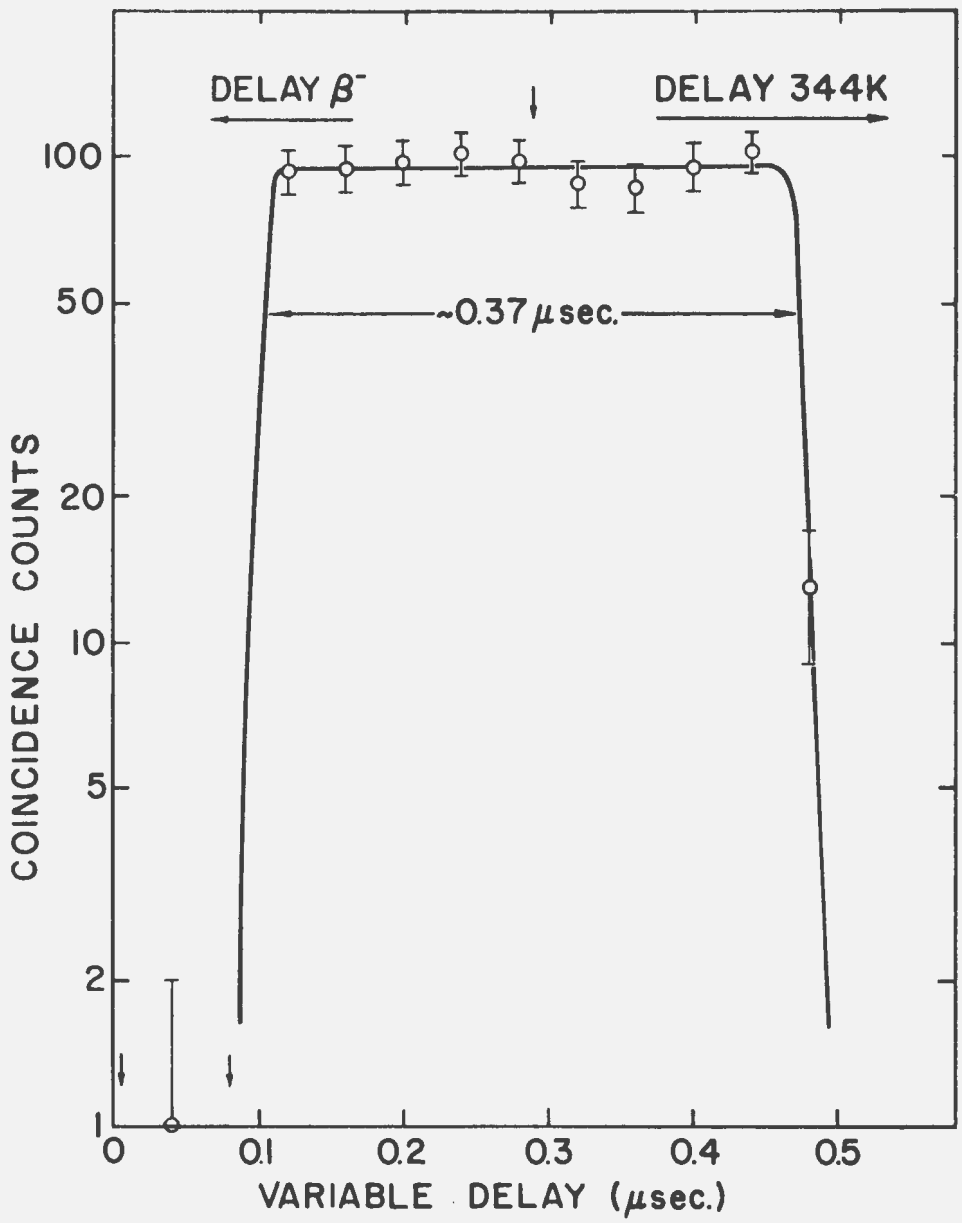

Fig. 9. Prompt coincidence curve between beta-rays and internal conversion electrons of the 344-kev transition in Gd^{152}.

trajectories are somewhat energy dependent as a result of the remanence or saturation effects in the iron yoke, the assumption that the solid angle or transmission is the same in both cases would be incorrect. Any significant energy dependence, however, should be seen as a deviation from the linear Kurie plot of allowed spectra. The performance of the spectrometers, in general, along this line has been thoroughly investigated by Nichols et al. (46) and in the present investigation a deviation of less than 0.5% from linearity between 75 and 200 kev was obtained for the Pm^{147} Kurie plot shown in Fig. 10. In addition, an energy dependent transmission should appear as a deviation from the linear relation between the current through the spectrometer coils and the momentum of the focused electrons. In this latter case a deviation of less than 0.3% was observed for the entire range of ThB calibration lines from 25 to 2500 kev. From these considerations it was estimated that the error contribution due to any variation of Ω_2 over the energy range of the 122 and 344 K-internal conversion lines would be less than 0.5%.

It should also be pointed out that since the same physical source was used for each relative measurement, no effects of the type described by Eq. 16 due to source size or position are present.

In determining the peak coincidences, $N_c(344)$ and $N_c(122)$, 4 or 5 points were taken across the peaks of the

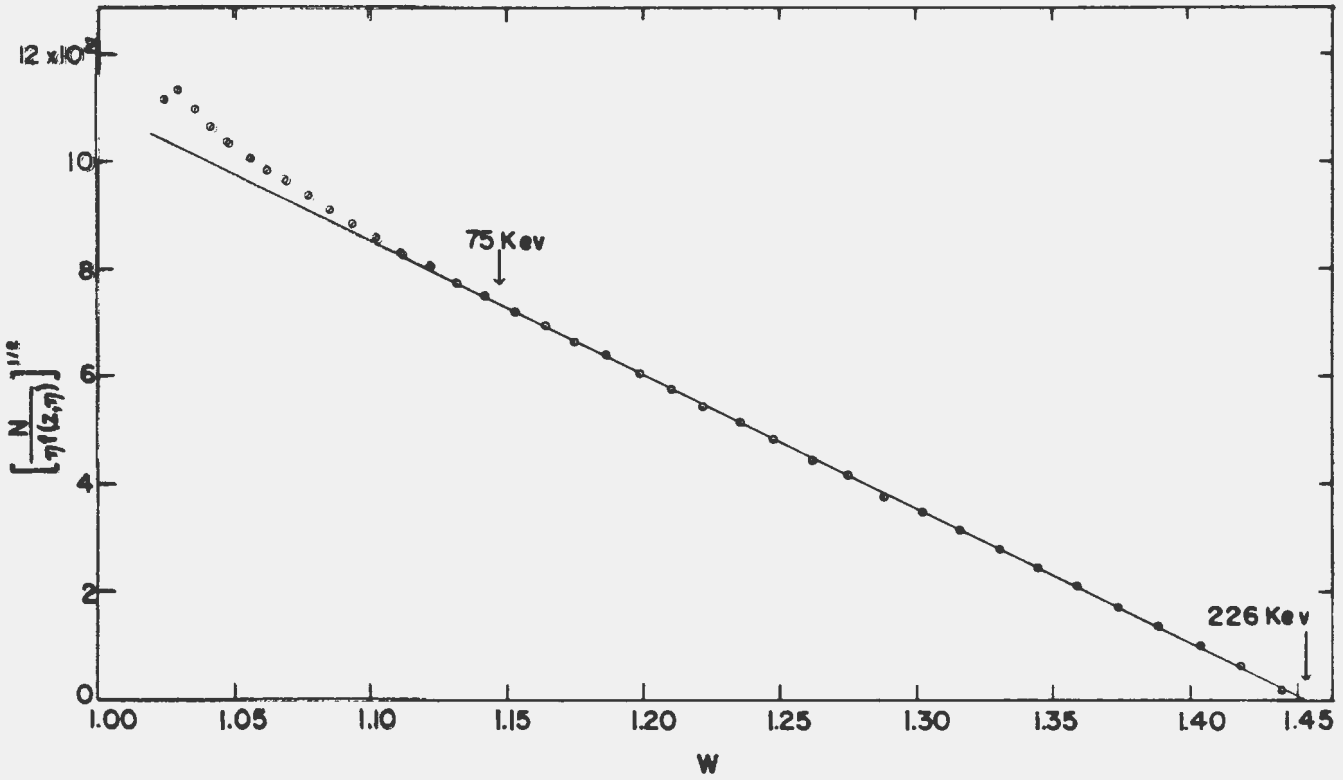

Fig. 10. Kurie plot of Pm^{147}.

internal conversion lines. Gaussian curves were then fitted to these points by the method of least squares. To allow for possible systematic errors, the error assignments were estimated to be approximately 1.5 times the statistical error of the combined number of true coincidences recorded across the peaks. Points taken away from the peaks, where no true coincidences were expected, showed very few or no coincidences above the calculated number of accidentals. The entire internal conversion spectra were run with Spec. 2 in the measurements of the α_K/α internal conversion ratios. These raw data were programmed through the Iowa State University IBM 650 computer whose output gave the values for the N/η and Kurie plots. Areas under the various peaks were then determined from the N/η spectra where the beta distributions under the peaks were estimated from the Kurie plots, and the peak heights were determined by fitting Gaussian curves to the upper points. The essentially Gaussian form of the line shapes can be seen in Figs. 11 and 12.

From the data shown in Fig. 11, the α_K/α ratio for the 344-kev transition was determined to be 0.786 ± 0.004. This value was obtained from both the coincidence and singles data, and the error assignment should easily cover systematic errors introduced by the background and 413 K-internal conversion line subtractions. The coincidence data shown in Fig. 11 were obtained with a beta scintillation spectrometer connected to Spec. 2 instead of the other intermediate-image spectrometer but were

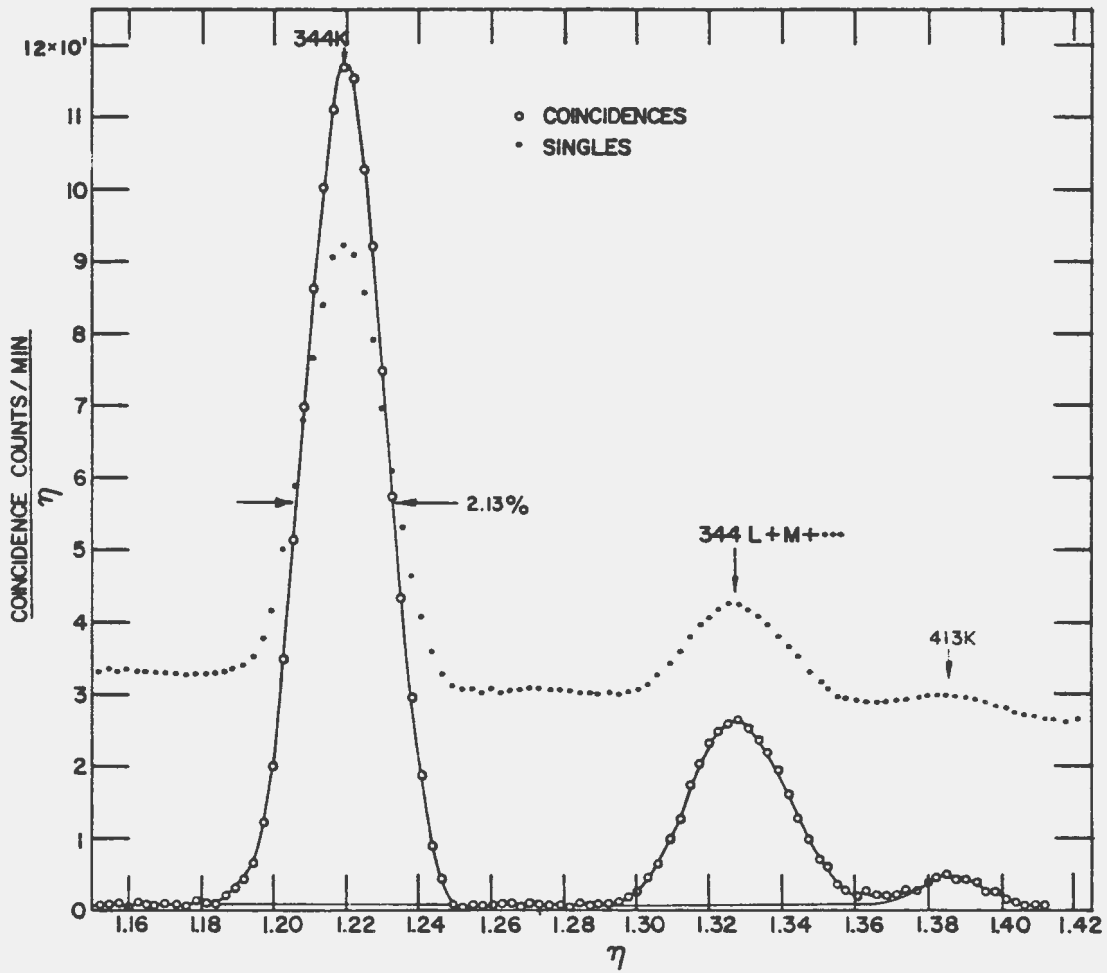

Fig. 11. Internal conversion-electron spectra of the 344-kev transition in Gd^{152} ($\eta = B\rho/mc$).

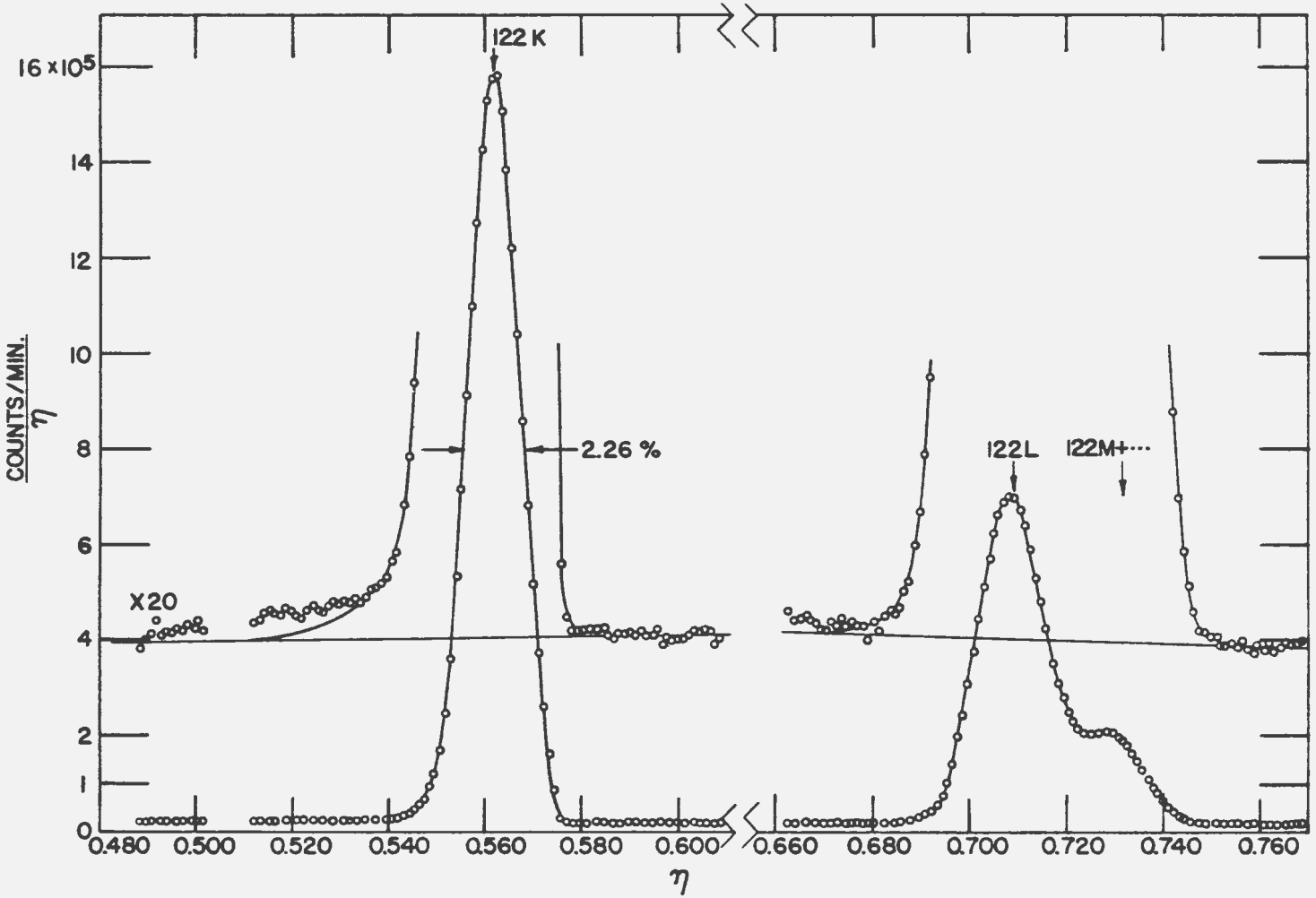

Fig. 12. Internal conversion-electron spectrum of the 122-kev transition in Sm^{152}.

not used in the internal conversion measurements because of the uncertainties which would be introduced by the change in experimental conditions with respect to the measurements on the 122-kev transition. The numerical result for the α_K/α ratio is in agreement with the value of 0.791 ± 0.003 calculated from the data of Bobykin and Novik (53).

The data from which the α_K/α value of 0.589 ± 0.003 was determined for the 122-kev transition is shown in Fig. 12. This value is in good agreement with the value of 0.590 ± 0.013 calculated from the data of Kelman *et al.* (54).

Since the linear Kurie plot discussed in connection with the possible energy dependent transmission effects suggests a constancy of the area under the N/η line shape rather than a constant peak height, the peak coincidences were normalized to the peak areas by using the area to peak ratios determined from the singles data. These ratios are discussed by Gerholm (36) and are approximately equal to the momentum resolution of Spec. 2 as can be seen from the values listed in Table II. Any source thickness effects would also be reduced by this procedure. In other experiments where source size and position effects are also important, the procedure of normalizing to the peak area reduces the possible errors caused by these effects as is discussed in Appendix A.

Using the formulas given by Wapstra *et al.* (55), the

fractions of 344 and 122 K-internal conversion electrons backscattered from the source were estimated to be 0.001 and 0.009 respectively. From the data of Wagner (56), however, essentially all of these backscattered electrons would be in the inelastically scattered regions below the observed peaks and therefore would not affect the coincidence or singles data across the peaks.

The fraction of total counts in Spec. 1 due to the 245 K-internal conversion line, $N_1(245K)$, was carefully determined from the total spectrum as shown in Fig. 13. The current value designated by the arrows in the figure was used rather than the peak value because any shift in the current control which would also change the beta background would easily be noticed. No irregularities of this type were noted in these runs, however. The smooth curve under the internal conversion lines of the 245-kev transition was estimated from a Kurie plot of the region shown.

The detection efficiencies, $\epsilon_2(344)$ and $\epsilon_2(122)$, were determined by displaying the pulse height spectra from the anthracene detector of Spec. 2 on an RCL 256-channel analyzer. Referring to the block diagram in Fig. 8, these pulses from the cathode follower output of the RCA 6810A photomultiplier were fed into the amplifier preceding the trigger to the coincidence circuit. The trigger pulses to the coincidence circuit, which were the pulses recorded on the No. 2 scaler,

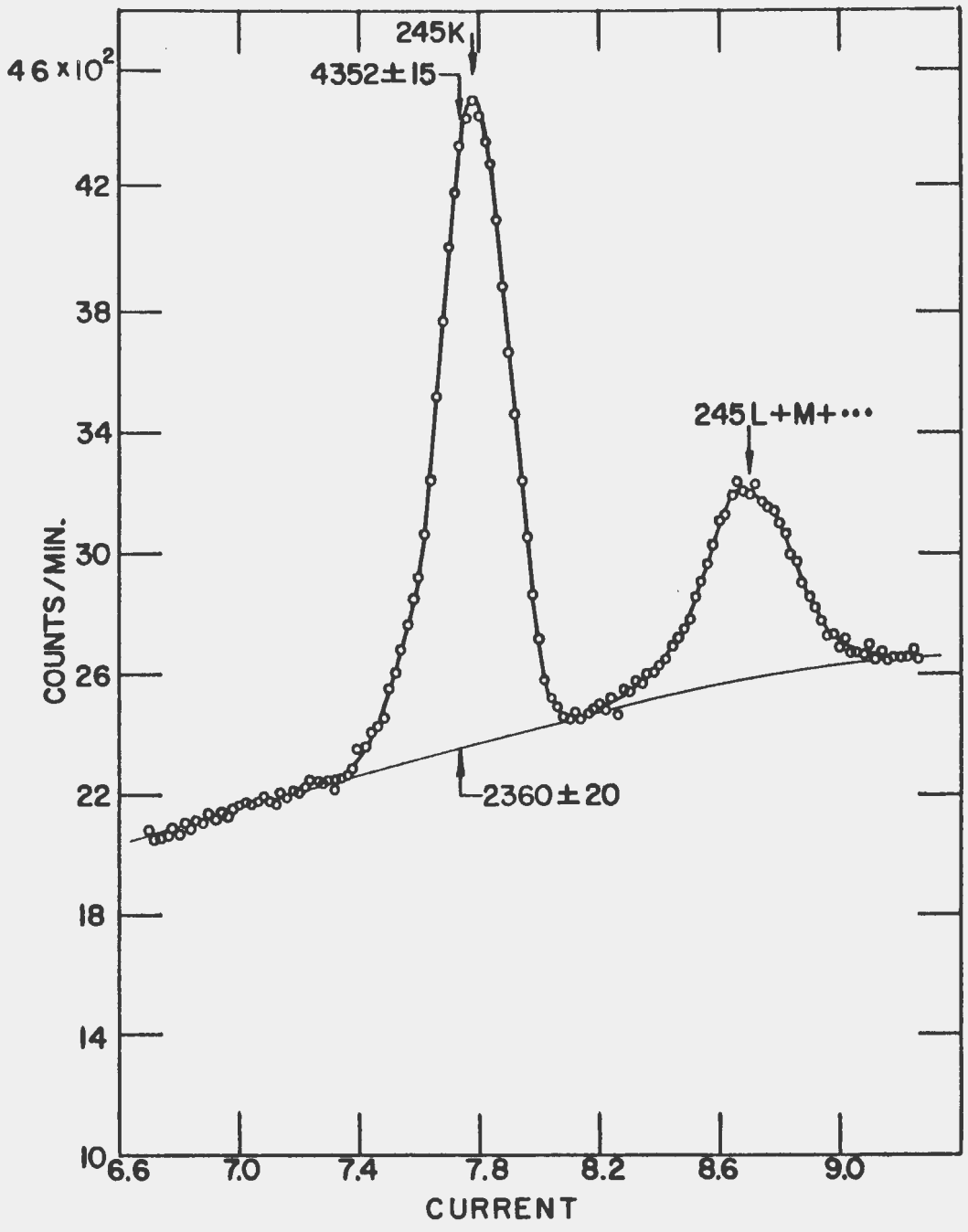

Fig. 13. Internal conversion-electron spectrum of the 245-kev transition in Sm^{152}.

were also used to gate the multichannel analyzer. The gated spectrum shown in Fig. 14 then differed from the total spectrum by not having the low energy pulses which were below the trigger level. A switch on the analyzer could open the gate momentarily in order to give the zero pulse height position. By extrapolating the tail of the distribution from the trigger level cutoff to the zero level, the fraction of counts lost and hence the efficiency could be estimated. Here again systematic errors may be present in the individual determinations but an error contribution from the $\epsilon_2(344)/\epsilon_2(122)$ ratio should be less than 0.2%.

The angular correlation factors, C(β-344) and C(245-122), are not known exactly, but estimates with appropriate error assignments can be made. Following the discussion presented in Appendix B, these factors can be calculated using the data of published gamma-ray angular correlation measurements in conjunction with estimated geometrical quantities for the coincidence spectrometer. The coefficient A_2 (A_4 assumed to be zero) has been measured between the 1.49-Mev beta-ray group and the 344-kev gamma ray (57,58) as a function of the higher beta-ray energies using $EuCl_3$ sources. When these results were extrapolated to 480 kev, A_2 was found to be -0.13 ± 0.03. This value combined with the 344-kev K-shell particle parameter and the fact that only half of the betas at 480 kev exhibit this angular correlation

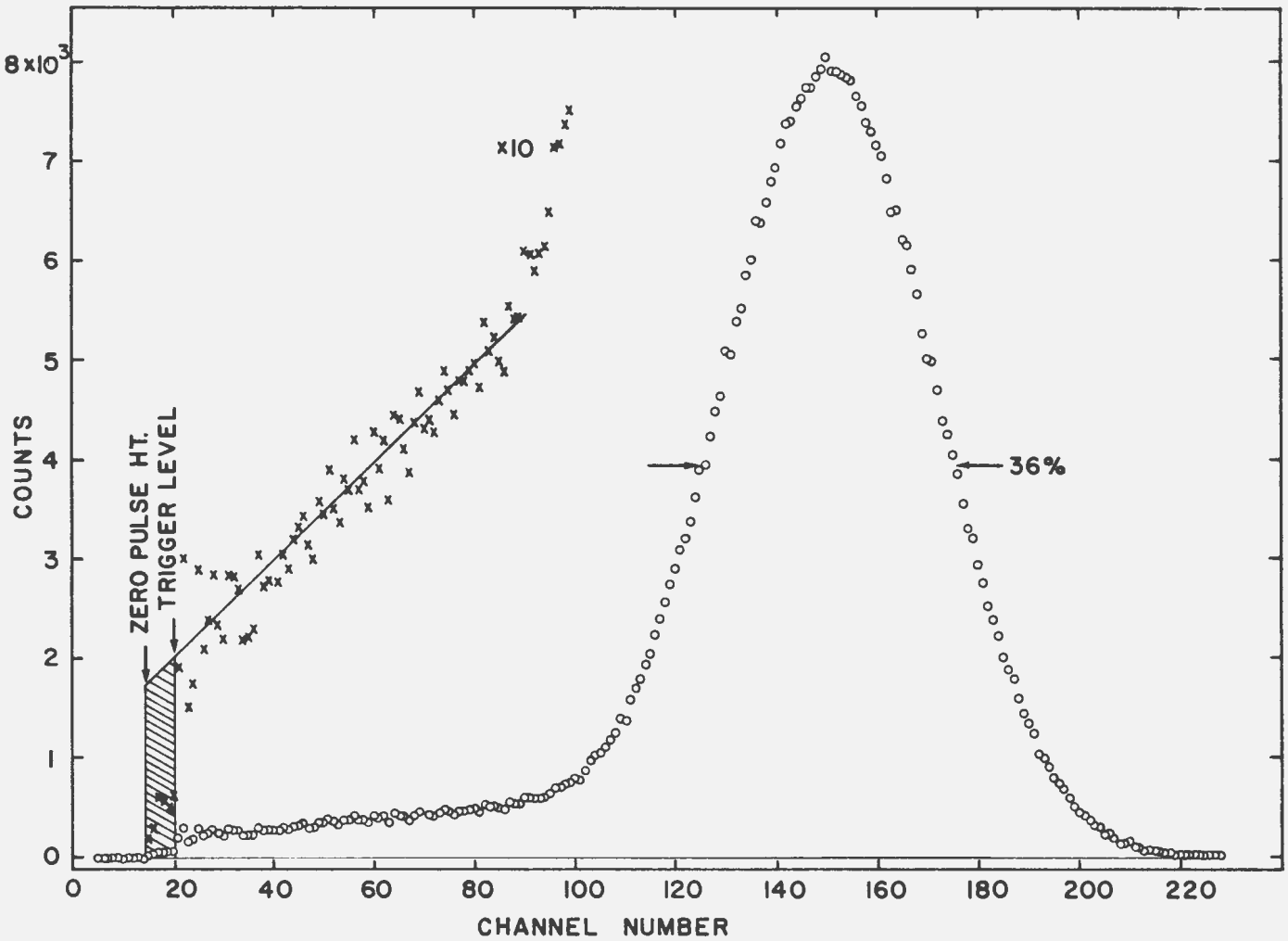

Fig. 14. Gated pulse height spectrum from the anthracene detector for 75-kev electrons (122 K-electrons).

effect gave the C(β-344) factor for the $EuCl_3$ data given in Table II. The same value of C(β-344) was also used for the data taken with the fluoride source because the half-life of the 344-kev level has been measured to be $(7.6 \pm 1.3)\times10^{-11}$ sec (59) and therefore any attenuation effects are expected to be small.

The coefficients A_2 and A_4 for the unattenuated angular correlation between the 245- and 122-kev gamma rays in Sm^{152} have been measured (60) to be 0.09 ± 0.01 and 0.01 ± 0.02, respectively, which corresponds to a value of 1.034 ± 0.014 for C(245-122). Since there are no experimental data for directly estimating the attenuation effects for the chloride and fluoride sources, an attenuation factor of 0.7 ± 0.2 was assumed for both of these sources to give the C factors listed in Table II. This assumption is in general agreement with the attenuation factor of 0.61 ± 0.03 obtained by Goldring and Scharenberg (61) for the angular distribution of the 122-kev gamma rays following Coulomb excitation in a solid $Sm_2^{152}O_3$ target and with the factor of 0.71 ± 0.03 obtained by Bhattacherjee and Mitra (62) for the 1277-123-kev gamma-gamma correlation in Gd^{154} using a solid $Eu^{154}Cl_3$ source.

Corrections were also made to the data for the 0.48% of Eu^{154} activity which was estimated to be in the enriched source. These corrections were simplified by the fact that

the K-internal conversion lines of the 245-kev transition in Sm^{152} and the 248-kev transition in Gd^{154} have the same energy. Ratios of the beta-ray intensities from the two activities at the energy settings of Spec. 1 were estimated from constructed N/η spectra. The multiplicative correction factors applied to $N_c(344)$ and $N_c(122)$ because of the Eu^{154} contaminant were 1.008 ± 0.003 and 1.000 ± 0.003, respectively.

An additional 344-kev measurement, which was not mentioned above, was made with the $EuCl_3$ source. The only reservation with taking these data relative to the 122-kev measurement on $EuCl_3$ discussed above is that the source had been removed from the spectrometer between the measurements. Source positioning effects due to simply removing and reinserting a source are expected to be quite small, however, and these data are also included in Table II.

Table II. Quantities used in the determination of $\alpha_K(344)$

Measurement	$(N_c/N_1)\times10^4$	(Area/Peak)	ϵ_2	C
β-344 ($EuCl_3$)	8.80 ±0.09	0.02237 ±0.00025	0.995 ±0.002	0.988 ∓0.005
245-122 ($EuCl_3$)	96.3 ±1.1	0.02385 ±0.00025	0.993 ±0.002	1.024 ±0.012
β-344 ($EuCl_3$)	8.70 ±0.10	a	0.997 ±0.001	a
β-344 (EuF_3)	8.70 ±0.10	0.02273 ±0.00025	0.999 ±0.001	0.988 ∓0.005
245-122 (EuF_3)	101.3 ±1.0	0.02380 ±0.00025	0.997 ±0.001	1.024 ±0.012

[a]The values used here were the same as those determined in the first $EuCl_3$ measurement.

V. RESULTS AND DISCUSSION

When the measured and calculated quantities of Table 2 are combined with the other experimental values given in the text, $\alpha_K(344)$ can be determined directly from Eq. 18. The error assignment for the present value is to be interpreted as a standard deviation and was derived by standard statistical methods from the individual error contributions. Comparisons with previously reported measurements and with the theoretical values are given in Table III. The theoretical values were determined by interpolations from a log k versus log α_K plot of the values given by Rose (27) and Sliv and Band (18).

Table III. α_K of the 344.3-kev transition in Gd^{152}

	$\alpha_K(344)$
Theoretical:	
Rose (27)	0.0313
Sliv and Band (18)	0.0310
Present work	0.0283[a] ± 0.0008
Hamilton et al. (63)	0.0281 ± 0.0020
Bhattacherjee et al. (64)	0.032 ± 0.005

[a]Relative to $\alpha_K(122) = 0.669 \pm 0.008$ (33).

The experimental value obtained for $\alpha_K(344)$ is in good agreement with the published results of Hamilton et al. (63) given in Table II and in better agreement with a revised value of 0.282 ± 0.0010.* It is also in general agreement with the trend discussed by Subba Rao (25) for measured internal conversion coefficients of E2 transitions in nearly spherical nuclei to be lower than the theoretical values. Possible contributions to the 9% discrepancy with theory are discussed below.

From the data of Bobykin and Novik (53) mentioned earlier, an α_L/α_K value of 0.209 ± 0.004 was calculated for the 344-kev transition. This value is in fair agreement with the theoretical value of 0.215 and can be combined with the present result for $\alpha_K(344)$ to give an $\alpha_L(344)$ value of 0.0059 ± 0.0002. The theoretical value (27) for $\alpha_L(344)$ is 0.0067.

The $\alpha_K(122)$ value of 0.669 ± 0.008 determined from the $\alpha(122)$ measurement of Lu and Schupp (52) is in very good agreement with its corresponding theoretical value of 0.677 (27,18). A 2% change in $\alpha_K(122)$ would change the $\alpha_K(344)$ result by approximately 1% in the same direction.

According to Rose (27), the error estimates for the

---

*Hamilton, J. H., Vanderbilt Univ., Nashville 5, Tenn. Recent investigations on E2 internal conversion coefficients. Private communication. 1962.

theoretical calculations should be at most 1% to 3% where dynamic effects are expected to be small. The lack of ambiguity in the theoretical calculations for $\alpha_K(344)$ is demonstrated by the fact that its value obtained by interpolation from the unscreened, point-nucleus calculations of Rose *et al.* (14) is less than 1% larger than the value of Rose quoted in Table III.

The differences between Rose's values (27) and the surface-current-model values of Sliv and Band (18) as estimated from the formalism of Rose (27) are less than 0.2% for the 344- and 122-kev transitions. Direct evaluation of the surface-current model values by interpolation from the tables of Sliv and Band give coefficients approximately 1% smaller than Rose's values as can be seen in Table IV. This difference between 1% and 0.2% then gives an indication of the errors introduced by interpolation as well as by the actual computer calculations.

A low energy approximation presented by Green and Rose (28,29) can be used to give further information concerning dynamic effects. As applied to E2 transitions it is possible to express a ratio of the K-internal conversion coefficients calculated from two different nuclear models in the form

$$\frac{\alpha_K(\Sigma)}{\alpha_K(\Sigma^o)} = 1 + \delta \quad , \tag{20}$$

where (Σ^o) refers to Sliv's surface current model which, as shown above, is nearly the same as Rose's no-penetration model for the 344- and 122-kev transitions. The δ is given

by $$\delta = - a x + b x^2 \quad , \tag{21}$$

where $$a = \frac{2}{1 + U_2^2}\left[U_2 \cos \tau_2 + \frac{\omega_{-3}}{b_o \omega_2}\right] \quad , \tag{22}$$

$$b = \frac{1}{1 + U_2^2} \quad , \tag{23}$$

and $$x = b_o \omega_2 \Sigma_{-3} \quad . \tag{24}$$

Green and Rose define (29) and tabulate (28,29) these parameters, but for the present discussion only the specific values for the 344- and 122-kev transitions are listed in Table IV. The variation of δ with respect to Σ_{-3} can then be considered, where

$$\Sigma_{-3} \approx \frac{5}{7} \frac{\int d\tau_N \rho_N Y_2^{M*} (r_N/R)^4}{\int d\tau_N \rho_N Y_2^{M*} (r_N/R)^2} \tag{25}$$

Substitution for the parameters in Eq. 21 gives

$$\delta (344) = -5.8 \times 10^{-4} \Sigma_{-3} + 7.5 \times 10^{-6} \Sigma_{-3}^2 \tag{26}$$

Table IV. Parameter values for the 344- and 122-kev transitions

	Transition 344	Transition 122
U_2	0.027	0.282
ω_2	0.0071	0.0054
ω_{-3}	0.00029	0.00016
$\overline{b_o}$	0.386	0.376
$\cos \tau_2$	0.0	-1.0
a	0.21	-0.37
b	1.00	0.93

and $$\delta\,(122) = 7.6\times10^{-4}\,\Sigma_{-3} + 3.8\times10^{-6}\,\Sigma_{-3}^{2} \quad . \qquad (27)$$

It can be seen from Eq. 26 that δ (344) has a minimum value of -0.01 with $\Sigma_{-3} = 39$, and it is therefore impossible for nuclear dynamic effects within this framework to give the -0.09 value for δ (344) needed to explain the experimental results. On the other hand, the experimental value of $\alpha_K(344)$ could be brought into agreement with theory by an increase in $\alpha_K(122)$. A δ (122) value of 0.20 would be required, however, which would correspond to $\Sigma_{-3} \approx 100$ in

Eq. 27. This 20% increase in $\alpha_K(122)$ is of course completely unjustified from an experimental viewpoint.

The large values above for Σ_{-3} which give a minimum value for δ (344) or a 0.20 value for δ (122) are also unexplainable from a theoretical point of view. In the expression for Σ_{-3} given in Eq. 25, the numerator would ordinarily be smaller than the denominator because of the (r_N/R) dependence so that the only way Σ_{-3} can be large is for the denominator to approach zero faster than the numerator. The denominator, however, is of the form of the matrix element for electric quadrupole gamma radiation involving a single proton (65) which certainly does not have the above behavior for the 344- and 122-kev transitions because their transition probabilities are enhanced over the single-proton values by factors of 20 (59) and 60 (66), respectively. Values for the quantities which correspond to Σ_{-3} above are discussed by Church and Weneser (20) for M1 and E1 transitions.

Considerations from the experimental measurement of $\alpha_K(344)$ which would tend to give slightly better agreement with theory include possible refinements to the decay scheme. Schneider (48) discussed a high energy, low intensity beta-ray group observed in his experiments on the beta decay of Eu^{152} but did not assign it definitely as a transition to the ground state of Gd^{152} because it would be 3rd forbidden

by beta decay selection rules. If the magnitude given by Schneider for this possible beta-ray group were used, $\alpha_K(344)$ would be increased by only 0.6%. Although neither has been reported, weak gamma rays of 1134 and 757 kev which would cross over the 344-kev level would also increase the present experimental value of $\alpha_K(344)$. From empirical half-life estimates (55) for these gamma rays, however, they are expected to be weaker than the 790- and 413-kev gamma rays, respectively, by factors of approximately 10^{11}.

While they apparently do not affect the reliability of the present $\alpha_K(344)$ measurement, intensities of beta-ray groups and cross-over gamma-ray transitions can limit the applicability of the electron-electron coincidence method for accurately determining internal conversion coefficients as is demonstrated by the measurements in Gd^{154} and Dy^{160} discussed in Appendix C.

Of all the statistical and systematic errors considered in this investigation, the largest was in estimating the ratio of the angular correlation factors, C(β-344)/C(245-122). The 1.7% error for this ratio comes principally from uncertainties in the electron trajectories and the angular correlation attenuation effects. Values given above and in Appendix B for these quantities are based on existing data and their corresponding error assignments are believed to be appropriate. Substantially better values

for these quantities could be determined only by involved experiments designed specifically for that purpose.

VI. CONCLUSION

In summarizing the results of this investigation, proper emphasis should be placed on the apparent 9% discrepancy between the experimental and theoretical values for $\alpha_K(344)$. Because of the experimental errors as well as small uncertainties in the theory, it is perhaps unwise to state that the observed discrepancy is more than 5%. On the other hand, a real 5% deviation from theory is significant since it is not explained theoretically. Support is given to the present experimental value by the agreement with the $\alpha_K(344)$ value measured by Hamilton et al. (63) who used a different method. It is in excellent agreement with a revised value by Hamilton.* This result, along with the observed trends for apparent discrepancies between experiment and theory for internal conversion coefficients of E2 transitions, then suggests that further investigations should be conducted on this class of transitions.

---

*Hamilton, J. H., Vanderbilt Univ., Nashville 5, Tenn. Recent investigations on E2 internal conversion coefficients. Private communication. 1962.

VII. REFERENCES

1. Gurney, R. W., Proc. Roy. Soc. (London) A109, 540 (1925).

2. Baeyer, O., O. Hahn and L. Meitner, Physik. Z. 12, 273 (1911).

3. Ellis, C. D. and W. A. Wooster, Proc. Roy. Soc. (London) A114, 276 (1927).

4. Swirles, B., Proc. Roy. Soc. (London) A116, 491 (1927).

5. Ellis, C. D. and G. H. Aston, Proc. Roy. Soc. (London) A129, 180 (1930).

6. Casimir, H., Nature 126, 953 (1930).

7. Hulme, H. R., Proc. Roy. Soc. (London) A138, 643 (1932).

8. Taylor, H. M. and N. F. Mott, Proc. Roy. Soc. (London) A138, 665 (1932).

9. Taylor, H. M. and N. F. Mott, Proc. Roy. Soc. (London) A142, 215 (1933).

10. Smekal, A., Z. Physik 10, 275 (1922).

11. Bainbridge, K. T., M. Goldhaber and E. D. Wilson, Phys. Rev. 90, 430 (1953).

12. Fisk, J. B. and H. M. Taylor, Proc. Roy. Soc. (London) A146, 178 (1934).

13. Curie, I. and M. F. Joliot, Compt. rend. 198, 254 (1934).

14. Rose, M. E., G. H. Goertzel, B. I. Spinrad, J. Harr and P. Strong, Phys. Rev. 83, 79 (1951).

15. Reitz, J. R., Phys. Rev. 77, 10 (1950).

16. Rose, M. E., Theory of Internal Conversion, in Siegbahn, K., ed., Beta- and Gamma-Ray Spectroscopy, pp. 396-413, 905-909 (Interscience Publishers, Inc., New York, N.Y., 1955).

17. Sliv, L. A., Zhur. Eksp. i Teoret. Fiz. 21, 770 (1951).

18. Sliv, L. A. and I. M. Band, U.S. Atomic Energy Commission Report AEC-tr-2888 [Technical Information Service Extension, AEC] (1957).

19. Wapstra, A. H. and G. J. Nijgh, Nuclear Phys. 1, 245 (1956).

20. Church, E. L. and J. Weneser, Phys. Rev. 104, 1382 (1956).

21. Nilsson, S. G. and J. O. Rasmussen, Nuclear Phys. 5, 617 (1958).

22. Asaro, F., F. S. Stephans, J. M. Hollander and I. Perlman, Phys. Rev. 117, 492 (1960).

23. Gerholm, T. R., B.-G. Pettersson, B. van Nooijen and Z. Grabowski, Nuclear Phys. 24, 177 (1961).

24. Church, E. L. and J. Weneser, Ann. Rev. Nuclear Sci. 10, 193 (1960).

25. Subba Rao, B. N., Nuovo cimento 17, 189 (1960).

26. Bernstein, E. M., Phys. Rev. Letters 8, 100 (1962).

27. Rose, M. E., Internal Conversion Coefficients (Interscience Publishers, Inc., New York, N.Y., 1958).

28. Green, T. A. and M. E. Rose, Phys. Rev. 110, 105 (1958).

29. Green, T. A. and M. E. Rose, U.S. Atomic Energy Commission Report ORNL-2395 [Oak Ridge National Laboratory, Tenn.] (1957).

30. McGowan, F. K. and P. H. Stelson, Phys. Rev. 107, 1674 (1957).

31. Hultberg, S. and R. Stockendal, Arkiv Fysik 14, 565 (1959).

32. Frey, W. F., J. H. Hamilton and S. Hultberg, Arkiv Fysik 21, 383 (1962).

33. Lu, D. C. and G. Schupp, Phys. Rev. [To be published ca. 1963].

34. Lu, D. C., Phys. Rev. 119, 286 (1960).

35. Taylor, J. G. V. and J. S. Merritt, Bull. Am. Phys. Soc Ser. 2 7, 352 (1962).

36. Gerholm, T. R., Arkiv Fysik 11, 55 (1956).

37. Feather, N., Proc. Cambridge Phil. Soc. 36, 224 (1940).

38. Feather, N., J. Kyles and R. W. Pringle, Proc. Phys. Soc. (London) 61, 466 (1948).

39. Siegbahn, K., Arkiv Fysik 4, 223 (1952).

40. Gerholm, T. R., Rev. Sci. Instr. 26, 1069 (1955).

41. Slätis, H. and K. Siegbahn, Arkiv Fysik 1, 339 (1949).

42. Slätis, H. and C. J. Herrlander, Rev. Sci. Instr. 26, 613 (1955).

43. Herrlander, C. J. and H. Slätis, Arkiv Fysik 20, 41 (1961).

44. Nichols, R. T., A. V. Pohm, J. H. Talboy, Jr. and E. N. Jensen, U.S. Atomic Energy Commission Report ISC-345 [Ames Lab., Ames, Iowa] (1953).

45. Nichols, R. T., A. V. Pohm, J. H. Talboy, Jr. and E. N. Jensen, Rev. Sci. Instr. 26, 580 (1955).

46. Nichols, R. T., R. E. McAdams and E. N. Jensen, Phys. Rev. 122, 172 (1961).

47. Schupp, G., H. Daniel, G. W. Eakins and E. N. Jensen, Phys. Rev. 120, 189 (1960).

48. Schneider, W., Nuclear Phys. 21, 55 (1960).

49. Way, K., N. B. Gove, C. L. McGinnis and R. Nakasima, Energy Levels of Nuclei, in Hellwege, K. H., ed., Landolt-Börnstein, New Series, Vol. 1, pp. 2-1 - 2-565 (Springer-Verlag, Berlin, Germany, 1961).

50. Scharff-Goldhaber, G. and J. Weneser, Phys. Rev. 98, 212 (1955).

51. Peker, L. K., Bull. Acad. Sciences U.S.S.R. 21, 1026 (1957).

52. Lu, D. C. and G. Schupp, Bull. Am. Phys. Soc. Ser. 2 7, 353 (1962).

53. Bobykin, B. V. and K. M. Novik, Bull. Acad. Sciences U.S.S.R. 21, 1546 (1957).

54. Kelman, V. M., V. A. Romanov, R. Ya. Metskhvarishvili and V. A. Kolyunov, Nuclear Phys. 2, 395 (1956).

55. Wapstra, A. J., G. J. Nijgh and R. van Lieshout, Nuclear Spectroscopy Tables (Interscience Publishers, Inc., New York, N.Y., 1959).

56. Wagner, P. R., Phys. Rev. 35, 98 (1930).

57. Sunier, J. W., D. Debrunner and P. Scherrer, Nuclear Phys. 19, 62 (1960).

58. Dulany, H., Jr., C. H. Braden and L. D. Wyly, Phys. Rev. 117, 1092 (1960).

59. Burde, J., M. Rakavy and S. Ofer, Phys. Rev. 124, 1911 (1961).

60. Lide, R. W. and M. L. Widenbeck, Phys. Rev. 113, 840 (1959).

61. Goldring, G. and R. P. Scharenberg, Phys. Rev. 110, 701 (1958).

62. Bhattacherjee, S. K. and S. K. Mitra, Phys. Rev. 126, 1154 (1962).

63. Hamilton, J. H., W. F. Frey, S. Hultberg and T. Duncan, Bull. Am. Phys. Soc. Ser. 2 6, 50 (1961).

64. Bhattacherjee, S. K., T. D. Nainan, S. Raman and B. Sabai, Nuovo cimento 7, 501 (1958).

65. Moszkowski, S. A., Theory of Multipole Radiation, in Siegbahn, K., ed., Beta- and Gamma-Ray Spectroscopy, pp. 373-395 (Interscience Publishers, Inc., New York, N.Y., 1955).

66. Sunyar, A. W., Phys. Rev. 98, 653 (1955).

67. Pettersson, B.-G., J. E. Thun and T. R. Gerholm, Nuclear Phys. 24, 243 (1961).

68. Huber, O., F. Humbel, H. Schneider, A. de Shalit and W. Zünti, Helv. Phys. Acta 24, 127 (1951).

69. Coburn, H. H., J. V. Kane and S. Frankel, Phys. Rev. 105, 1293 (1957).

70. Frauenfelder, H., Angular Correlation, in Siegbahn, K., ed., Beta- and Gamma-Ray Spectroscopy, pp. 531-599 (Interscience Publishers, Inc., New York, N.Y., 1955).

71. Franklin, P., Basic Mathematical Formulas, in Menzel, D. H., ed., Fundamental Formulas of Physics, pp. 1-106 (Prentice-Hall, Inc., New York, N.Y., 1955).

72. Juliano, J. O. and F. S. Stephans, Jr., Phys. Rev. 108, 341 (1957).

73. Grigor'ev, E. P., A. V. Zolotavin and B. Kratsik, Bull. Acad. Sciences U.S.S.R. 23, 183 (1959).

IX. APPENDIX A: SOLID ANGLE MEASUREMENTS

If absolute measurements of internal conversion coefficients are to be made with a lens spectrometer, it is necessary to know its solid angle. The solid angle or transmission will depend on the baffle settings as well as source size and position. It is therefore important that any solid angle measurements be performed under the same experimental conditions as the primary experiment.

Consider a simple nuclear level scheme of the form shown in Fig. 15A and let the transitions be denoted by T2 and T1. If these transitions have at least moderate internal conversion coefficients ($\alpha > 0.1$), then a coincidence measurement of the form described by Eqs. 17 and 18 can be performed. Referring again to the block diagram of Fig. 8 and supposing that the solid angle of Spec. 2 is to be measured, if Spec. 1 is set on an internal conversion line of T1 then each of these electrons detected would be in coincidence with T2. With Spec. 2 set on the peak of the K-internal conversion line of T2, the number of coincidence counts, $N_c(2)$, would be given by

$$N_c(2) = N_1(1)[1+\alpha(2)]^{-1}\alpha_K(2)\Omega_2\epsilon_2(2)\epsilon(\text{coin})C(1\text{-}2) \quad , \quad (28)$$

where the 1 and 2 subscripts refer to Specs. 1 and 2 and the numbers in parentheses refer to T1 and T2. It is convenient

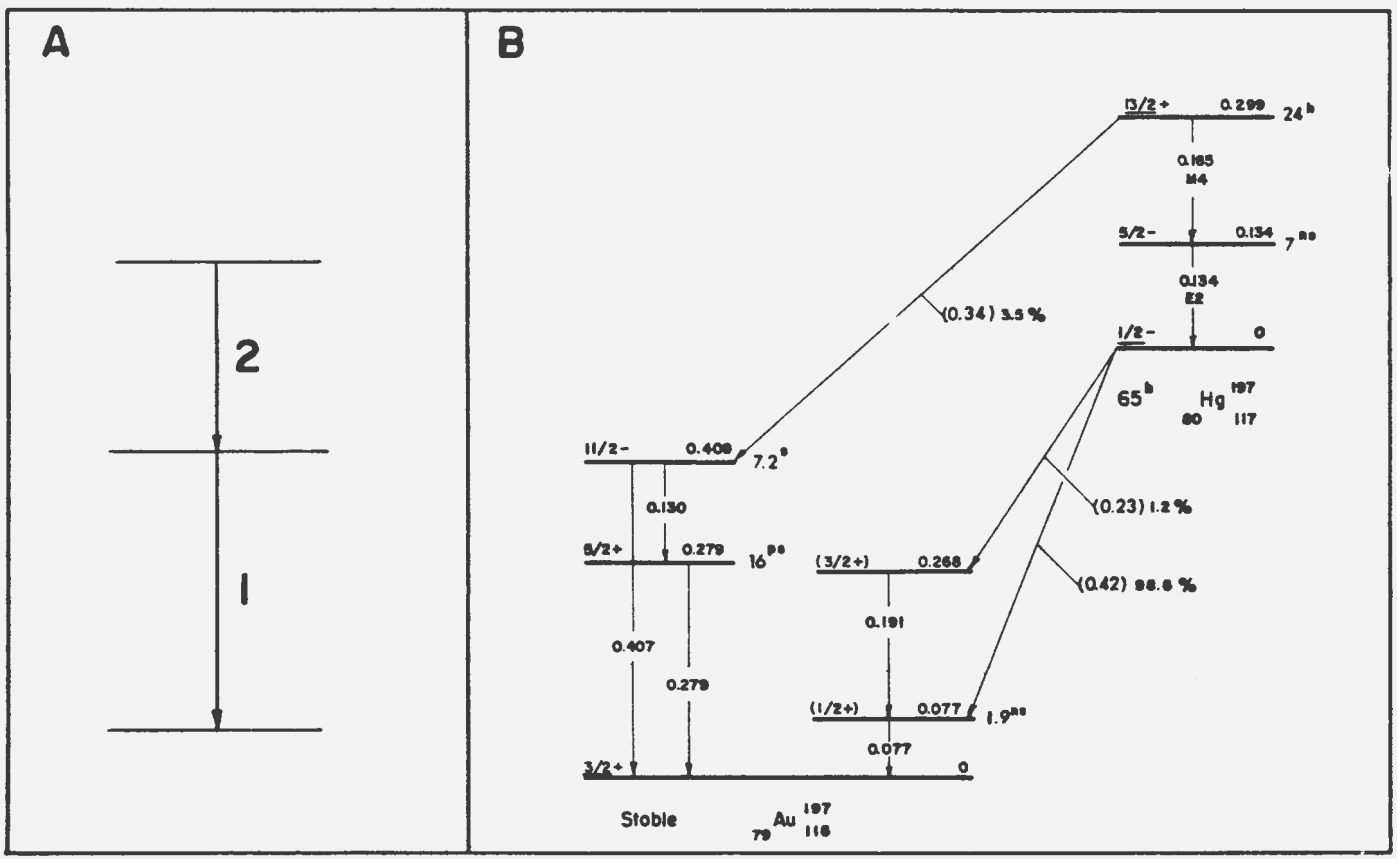

Fig. 15A. Simple nuclear level scheme.

Fig. 15B. Decay scheme of Hg^{197m}.

to group ϵ(coin) with Ω_2 and to denote the combined quantity by (Ω_2) which can then be determined from

$$(\Omega_2) = \frac{N_c(2)}{N_1(1)} \left[\frac{1}{\alpha_K(2)} + \frac{\alpha(2)}{\alpha_K(2)}\right] \frac{1}{\epsilon_2(2)} \frac{1}{C(1-2)} \quad . \qquad (29)$$

The usefulness of this method as a means of determining (Ω_2) absolutely then depends upon $\alpha_K(2)$ being a large number such that any uncertainties in its value would not add an appreciable error. Although advantageous here, this insensitivity to large values of α_K is reflected in the large errors for the measurements discussed in Appendix C. If the angular correlation factor can be estimated to a satisfactory degree of accuracy as discussed in Appendix B, the remaining quantities in Eq. 29 can usually be measured to accuracies such that the overall error on (Ω_2) is 2% or smaller.

Several nuclear isomers fulfill the necessary requirements of the simple decay scheme and large $\alpha_K(2)$ but for most of them it is difficult to obtain and prepare a satisfactory source for the spectrometer. The Hg^{197m} isomer was chosen for this measurement and was obtained as a stock item from the Oak Ridge National Laboratory; its decay scheme (49) is shown in Fig. 15B. A correspondence is made between the 165- and 134-kev transitions in Hg^{197} and T2 and T1 of the preceding discussion.

The source was vacuum evaporated from the chloride

form in the manner described earlier. A major difficulty encountered with this source was the growth of the M-internal conversion electrons from the 77-kev transition in Au^{197} which dominated the singles spectrum in the region of the 165 K-internal conversion line. The 165 K-internal conversion line obtained in coincidence with the 134 L-internal conversion line is shown in Fig. 16 along with the singles spectrum of the remaining internal conversion lines of the 165-kev transition. A measurement of the $\alpha_K(165)/\alpha(165)$ ratio was then made by also taking coincidence data across the peak of the 165 L-internal conversion line. The value obtained for this ratio was 0.226 ± 0.012 compared with the values of 0.207 and 0.242 calculated from the data of Pettersson et al. (67) and Huber et al. (68), respectively. The errors on these two values are expected to be $\approx 5\%$. Coburn et al. (69) have measured $\alpha(165)$ to be 350 ± 90.

In parallel with the description of the internal conversion measurements, the remaining quantities used in the determination of (Ω_2) are given in Table V. The angular correlation factor, C(134-165), was estimated from the measurements of Coburn et al. (69) in conjunction with the discussion given in Appendix B. An attenuation factor of 0.4 ± 0.2 was used for the solid $Hg^{197m}Cl_2$ source.

From the values listed, $(\Omega_2)_A$ was calculated to be $(7.54 \pm 0.58) \times 10^{-4}$ 4π steradians. This value is for the

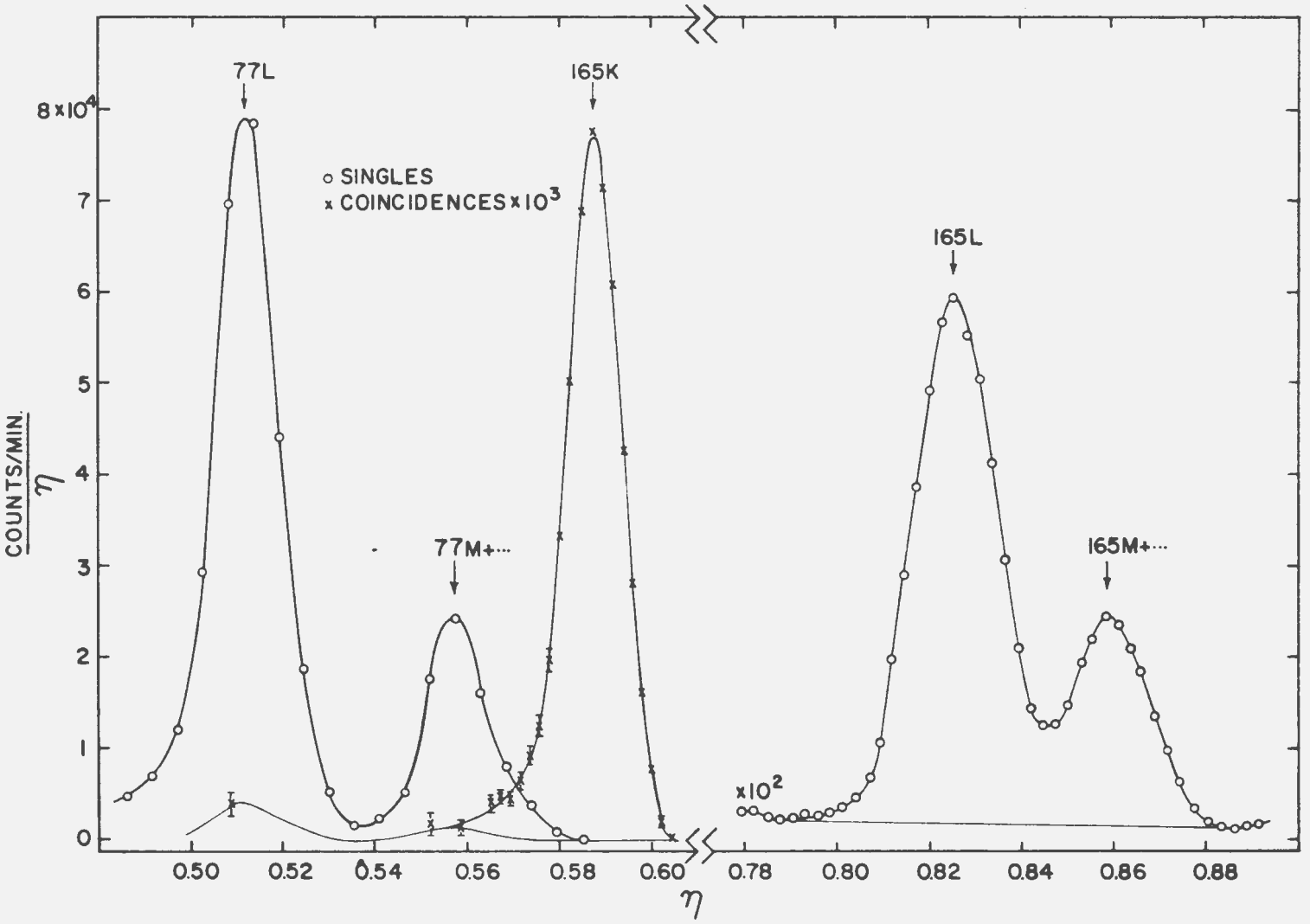

Fig. 16. Internal conversion-electron spectra of the 165-kev transition in Hg^{197}.

Table V. Quantities used in the determination of (Ω_2)

Measurement	$(N_c/N_1)\times10^3$	(Area/Peak)	ϵ_2	C(134-165)
134-165 $HgCl_2$	6.51 $\pm$0.10	0.0264 $\pm$0.0014	0.995 $\pm$0.002	1.015 $\pm$0.010

transmission of Spec. 2 based on the area under the internal conversion peak rather than on the peak height directly. The value for $(\Omega_2)_P$ based only on the peak height from these measurements without including additional systematic errors is $(2.85 \pm 0.16)\times10^{-2}$ 4π steradians. Values of $(\Omega_2)_A$ and $(\Omega_2)_P$ calculated from the measurements on the 122-kev transition in Sm^{152} are $(7.38 \pm 0.13)\times10^{-4}$ and $(3.10 \pm 0.05)\times10^{-2}$ 4π steradians based on the peak area and peak height, respectively. A comparison of the $(\Omega_2)_A$ and $(\Omega_2)_P$ values indicates that source size and position effects are better accounted for by using the peak areas rather than the peak heights.

The difficulties which arose in this experiment due to the Hg^{197} 65-hour activity could be overcome with a fresher source but because of the inherent delay in getting a source from the Oak Ridge National Laboratory no further solid angle measurements were made.

X. APPENDIX B: ANGULAR CORRELATION FACTORS

Whenever coincidence measurements are made between nuclear radiations, angular correlation effects may be present and must be assessed for any particular experiment. In this discussion the angular correlation effects arising from coincidences between the radiations detected in the electron-electron coincidence spectrometer are considered.

The geometrical orientation of the electron trajectory through the spectrometers is shown schematically in Fig. 17. The angles which are used in the discussion below are given in the figure; CB 1 and CB 2 represent the center baffles for Specs. 1 and 2, respectively, which define the intermediate images. To formulate the calculation, it is assumed that the only electrons detected in the spectrometers leave the point source at S in the axial symmetric angular regions $\Delta\theta_1$ and $\Delta\theta_2$. It is further assumed that the detection probability is unity for electrons leaving the source in these angular regions and is zero otherwise.

Consider again the simple level scheme in Fig. 15A, and let the electrons from T1 be focused in Spec. 1 and from T2 in Spec. 2. The number of coincidences will then be given by

$$N_c = N_o K \int_1 \int_2 [d\Omega_1/4\pi] [d\Omega_2/4\pi] W(\phi) \quad , \qquad (30)$$

where N_o is the total number of decays and K is a propor-

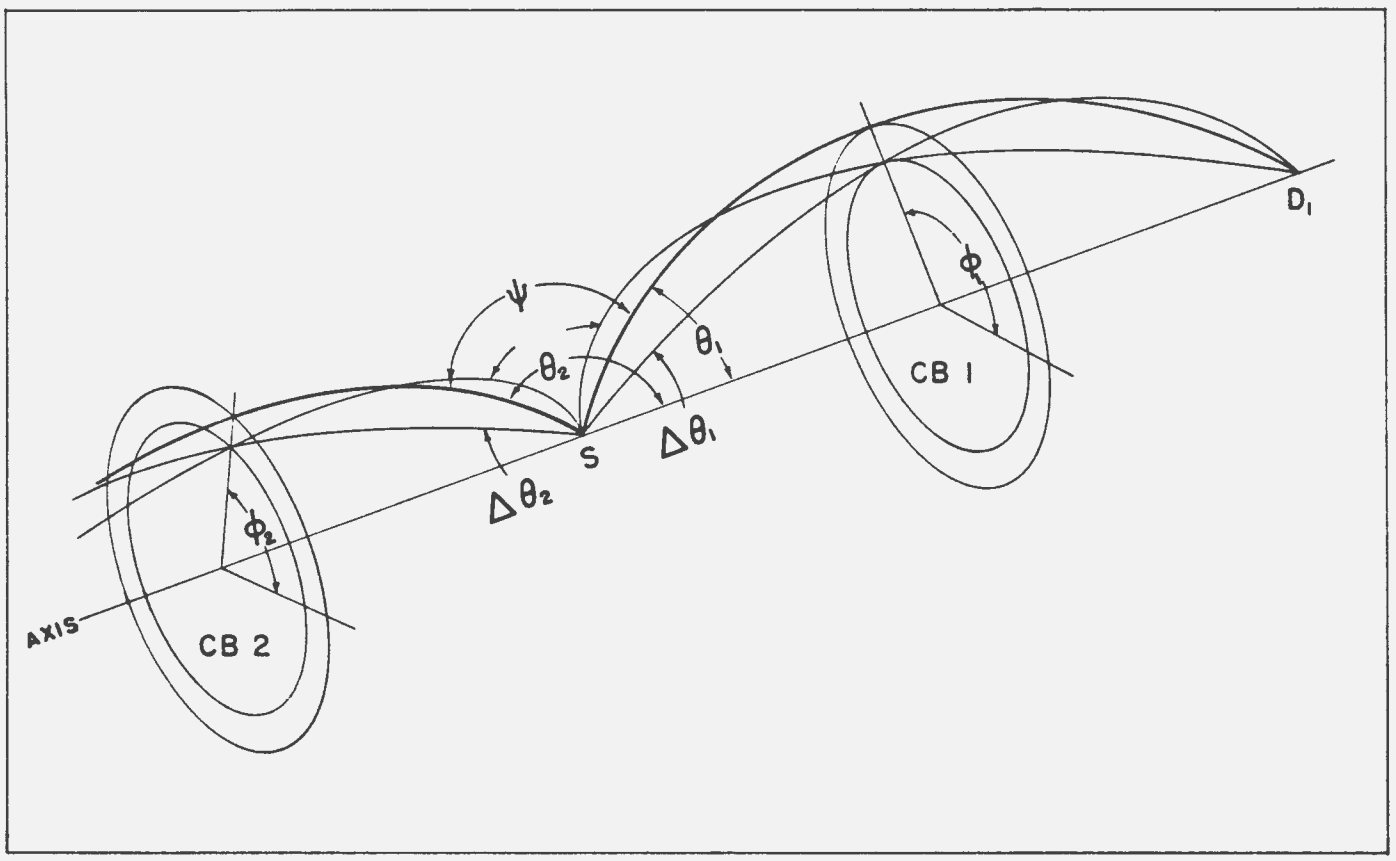

Fig. 17. Schematic drawing of the electron trajectories through the spectrometers.

tionality constant dependent upon the internal conversion coefficients of the transitions. The quantities $[d\Omega_1/4\pi]$ and $[d\Omega_2/4\pi]$ integrated over the angular regions $\Delta\theta_1$ and $\Delta\theta_2$, respectively, give the fractions of the total number of T1 and T2 internal conversion electrons detected. $W(\psi)$ is the angular correlation function which expresses the relative probabilities for coincidences between electrons that leave the source at an angle ψ with respect to each other. It has the form (70)

$$W(\psi) = \sum_{n \text{ even}} b_n(1)\, b_n(2)\, A_n\, P_n(\cos\psi) \quad , \qquad (31)$$

where $b_n(1)$ and $b_n(2)$ are particle parameters for the electrons detected in Specs. 1 and 2, respectively; A_n are the usual expansion coefficients for gamma-gamma directional angular correlation measurements; and P_n are Legendre polynomials.

For application to the experimental geometry, it is convenient to expand $P_n(\cos\psi)$ (71) in terms of the angles θ_1, ϕ_1 and θ_2, ϕ_2 to give

$$\begin{aligned} P_n(\cos\psi) &= P_n(\cos\theta_1)\, P_n(\cos\theta_2) \\ &\quad + 2 \sum_{m=1}^{n} \frac{(n-m)!}{(n\ m)!}\, P_n{}^m(\cos\theta_1)\, P_n{}^m(\cos\theta_2)\, \cos m(\phi_1-\phi_2). \end{aligned} \qquad (32)$$

Since the terms with ϕ_1 and ϕ_2 vanish when integrated from

0 to 2π, the final result for N_c, following the substitutions and integrations, is

$$N_c = N_o K [\Omega_1/4\pi] [\Omega_2/4\pi] \cdot \sum_{n \text{ even}} b_n(1)\, b_n(2)\, A_n\, \overline{P_n(\cos\theta_1)}\, \overline{P_n(\cos\theta_2)} \quad , \qquad (33)$$

where $\overline{P_n(\cos\theta_1)}$ is the average of $P_n(\cos\theta_1)$ over the angular region $\Delta\theta_1$.

In the internal conversion coincidence measurements, the angular correlation factor, C(1-2), is then given by

$$C(1\text{-}2) = \sum_{n \text{ even}} b_n(1)\, b_n(2)\, A_n\, \overline{P_n(\cos\theta_1)}\, \overline{P_n(\cos\theta_2)} \quad . \qquad (34)$$

To calculate the $\overline{P_n}$ terms, the angular regions $\Delta\theta_1$ and $\Delta\theta_2$ must be determined from the experimentally measured values of θ_1 and θ_2, and the corresponding estimates of the solid angles Ω_1 and Ω_2 . The angles of the primary rays, θ_1 and θ_2, have been measured to be 42° and 138°, respectively. These values are only accurate to 2° , however, and thereby introduce large errors in the $\overline{P_n}\ \overline{P_n}$ products which are discussed below.

In all of the internal conversion experiments performed in this investigation, the baffles of Spec. 2 were never changed and its solid angle was measured to be 3% of 4π steradians. Combining this value with θ_2 limits $\Delta\theta_2$ to

the angles between 141° and 136°. Two baffle settings of Spec. 1 were used in the experiments depending upon whether it was detecting internal conversion electrons or beta rays. For internal conversion electron detection, $\Delta\theta_1$ was defined by the angles 38° and 45°; $\Delta\theta_1$, for beta-ray detection, was defined by the angles 37° and 46°. These values for $\Delta\theta_1$ correspond to θ_1 and estimated solid angles of 4% and 5% of 4π steradians for Spec. 1. Differences in the values for $\overline{P_n}$ calculated from the different $\Delta\theta_1$ were only about 1% and the average values used for the products $\overline{P_2(\cos\theta_1)}\ \overline{P_2(\cos\theta_2)}$ and $\overline{P_4(\cos\theta_1)}\ \overline{P_4(\cos\theta_2)}$ of Eq. 34 were 0.115 and 0.122, respectively. Systematic errors in these numbers due to the uncertainties in θ_1 and θ_2 mentioned above are ~40% and in some cases could severely limit the accuracy of an entire coincidence measurement.

Theoretical values of A_n are tabulated (55), but in calculating C(1-2) the experimental values reported in the literature from gamma-ray angular correlation measurements were used. Values of b_n are also tabulated (55) for K-shell internal conversion electrons, and those used in this investigation are listed in Table VI. The explicit form used for estimating C(1-2) is then

$$C(1\text{-}2) = 1 + (0.115 \pm 0.045)\, b_2(1)\, b_2(2)\, A_2 + (0.12 \pm 0.05)\, b_4(1)\, b_4(2)\, A_4 \quad . \qquad (35)$$

Table VI. Values for the particle parameters b_n

n	$b_n(344)$	$b_n(122)$	$b_n(245)$	$b_n(165)$	$b_n(134)$	$b_n(123)$
2	1.59	1.89	1.71	1.07	1.87	1.89
4	----	-1.22	-0.78	1.38	-1.18	----

Attenuation effects due to source environment are discussed in the text along with the experimental values for A_n. In practice, the signs of the A_2 coefficients determine whether the large systematic errors introduced by the $\overline{P_2}\ \overline{P_2}$ product will add or subtract when a ratio of C factors is taken. For example, in the $C(\beta\text{-}344)/C(245\text{-}122)$ ratio the opposite signs for the A_2's contribute to a 1.7% error which is the largest single source of error in the relative measurement of $\alpha_K(344)$ to $\alpha_K(122)$.

XI. APPENDIX C: INTERNAL CONVERSION MEASUREMENTS IN Gd^{154} AND Dy^{160}

In addition to the primary experimental investigation presented above, internal conversion coefficient measurements were also performed on the 123- and 87-kev, E2 transitions in Gd^{154} and Dy^{160}, respectively, and are described below.

A. Measurements in Gd^{154}

The decay of Eu^{154} leads to the levels of Gd^{154} according to the decay scheme shown earlier in Fig. 7. A sample of enriched (95%) $Eu_2^{153}O_3$ was irradiated by slow neutrons in a reactor at the Oak Ridge National Laboratory to produce the Eu^{154} activity used in this investigation. Preparation of the $Eu^{154}F_3$ source for the spectrometer and the actual measurement of the internal conversion coefficient of the 123-kev transition was performed in a manner exactly analogous to the measurement on the 344-kev transition described above. Two additional complications arose in this experiment, however, due to approximately 25% of Eu^{152} activity contained in the source and to the fact that all of the beta-ray transitions do not lead to the 123-kev level.

If Spec. 1 is set on the beta distribution at an energy of 163 $\pm$ 8 kev, the number of coincidences obtained by

setting on the peak of the 123 K-internal conversion line in Spec. 2 is given by

$$N_c(123) = R(163)\, N_1(\beta)\, f(163)\, [1 + \alpha(123)]^{-1}\, \alpha_K(123) \cdot (\Omega_2)\, \epsilon_2(123)\, C(\beta - 123) \quad , \tag{36}$$

where R(163) is the ratio of the Eu^{154} betas to the total number of betas at 163 kev, and f(163) is the fraction of Eu^{154} betas at 163 kev which lead to the 123-kev transition. The other symbols are the same as those used previously, and the peak height value of $(3.10 \pm 0.05)\times10^{-2}$ 4π steradians discussed in Appendix A was used for $(\Omega_2)_p$. This value was used rather than the one based on the peak area because the true shape of the 123 K-internal conversion line was not known and because any systematic errors introduced by an energy dependence of Ω_2 would be negligible in this case.

The internal conversion lines of the 123-kev transition are shown in Fig. 18 with the contaminant from the 122-kev transition. From these data and the α_K/α ratio for the 122-kev transition, the α_K/α ratio for the 123-kev transition was determined to be 0.531 ± 0.007. This value is changed only 0.3% by a 10% change in the amount of the contaminant. For comparison, a value of 0.553 ± 0.010 was estimated from the data of Kelman *et al.* (54) by assuming an $\alpha_L/\alpha_{M+\ldots}$ ratio of 4.5 ± 0.9. This assumption is based on the 4.5 ± 0.1 value for the same ratio of the 122-kev transition

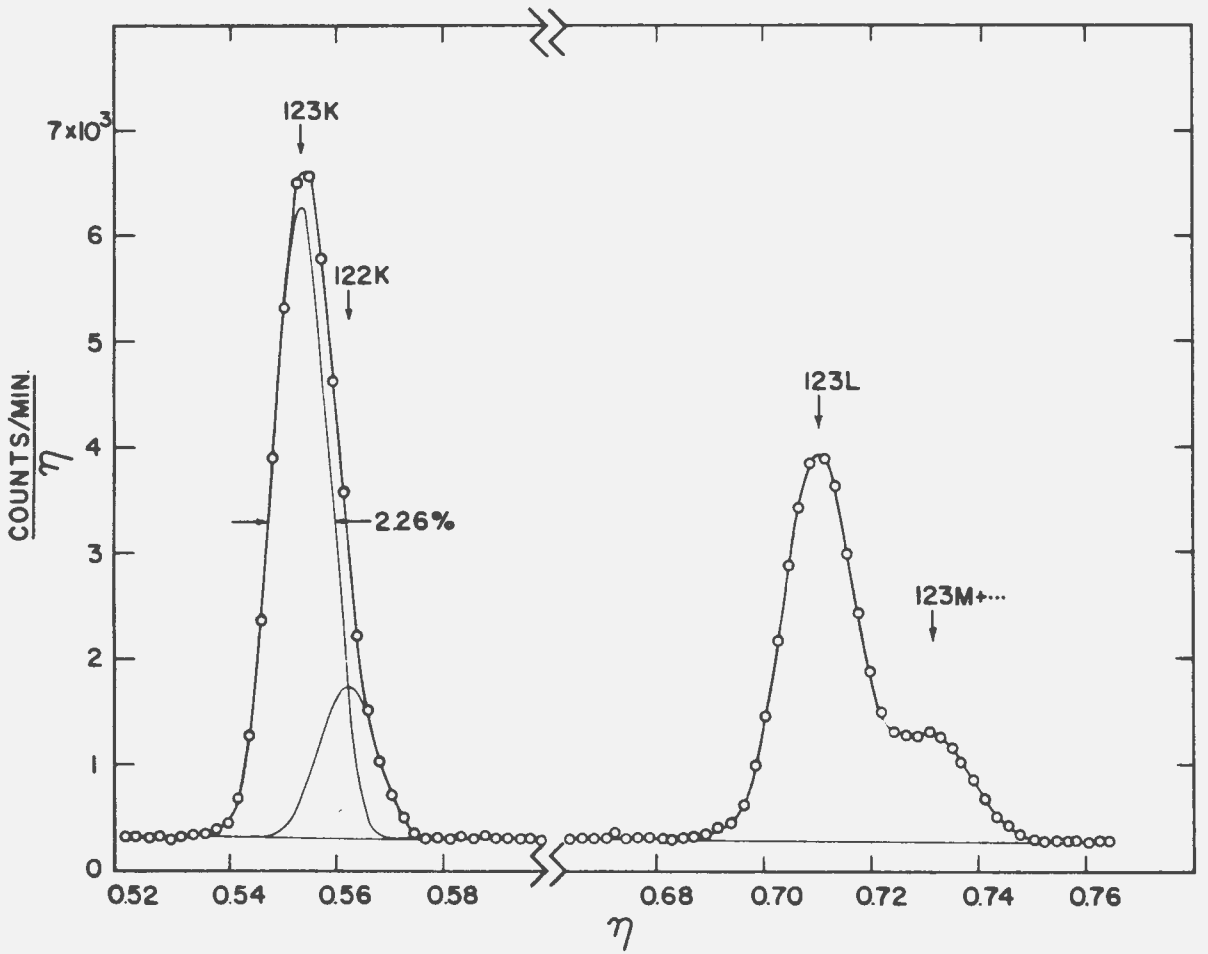

Fig. 18. Internal conversion-electron spectrum of the 123-kev transition in Gd^{154}.

which was also measured by them.

An experiment with Spec. 1 set at 163 ± 8 kev gave an unexpectedly low value for $\alpha_K(123)$ and a repeat experiment was subsequently performed. An additional measurement was also performed with Spec. 1 set at 480 ± 25 kev where the R and f factors of Eq. 36 would be different from those at 163 kev. The R factors were estimated from N/η beta spectra constructed according to the Eu^{154} and Eu^{152} decay schemes and were adjusted by the number of 344 K-internal conversion electrons; the f factors were estimated from the decay scheme branching ratios and the N/η beta spectrum of Eu^{154}.

Extrapolation of the beta-gamma directional correlation measurements in Eu^{154} by Bhattacherjee and Mitra (62) to 163 and 480 kev gave values of -0.02 ± 0.01 and -0.07 ± 0.02, respectively, for the A_2 coefficients which were used in estimating the angular correlation factors discussed in Appendix B. The measured and estimated quantities for these experiments are listed in Table VII

Values of $\alpha_K(123)$ calculated from the quantities listed in Table VIIand in the text give the results tabulated in Table VIII. The errors on the experimental values of $\alpha_K(123)$ come primarily from the R and f factors which limit the accuracy of these measurements.

The fact that the beta-group intensities total 100% introduces systematic tendencies which would cause the value

Table VII. Quantities used in the determination of $\alpha_K(123)$

Beta energy	$(N_c/N_1)\times10^4$	ϵ_2	R	f	C
163	68.6 ± 0.8	0.990 ± 0.004	0.905	0.890	1.000
	69.6 ± 0.8	0.995 ± 0.002	±0.018	±0.018	±0.001
480	73.4 ± 0.8	0.995 ± 0.002	0.836	0.940	0.996
			±0.028	±0.010	∓0.002

Table VIII. α_K of the 123.1-kev transition in Gd^{154}

	$\alpha_K(123)$
Theory (27)	0.650 ± 0.010
Present measurements:	
163	0.590 ± 0.045
480	0.715 ± 0.065
Average	0.65 ± 0.07
Juliano and Stephans (72)	0.54 ± 0.14
Bernstein (26)	0.82[a] ± 0.12

[a]Calculated from $\alpha(123) = 1.46 \pm 0.20$.

of N_1 (β) to be low at 480 kev if it were high at 163 kev. These tendencies would then lend support to the average value for $\alpha_K(123)$ given in Table VIII and its apparent agreement with theory even though it is derived from two widely different values. These different values indicate that additional investigations should be conducted on the Eu^{154} beta decay.

Although the good agreement with theory for the average value discussed above is somewhat fortuitous and should not be overemphasized, the individual values for $\alpha_K(123)$ are still in better agreement with theory than the other published values.

B. Measurements in Dy^{160}

The sample used in this investigation was produced by slow neutron irradiation of the 100% isotope of $Tb_4^{159}O_7$ in a reactor at the Oak Ridge National Laboratory. Preparation of the fluoride source and the other experimental procedures followed were exactly the same as those described above.

Considering the abbreviated decay scheme of Tb^{160} (49) shown in Fig. 19, if Spec. 1 is set on the beta distribution at an energy of 345 $\pm$ 15 kev, the number of coincidences obtained by setting on the peak of the 87-kev K-internal conversion line in Spec. 2 is given by

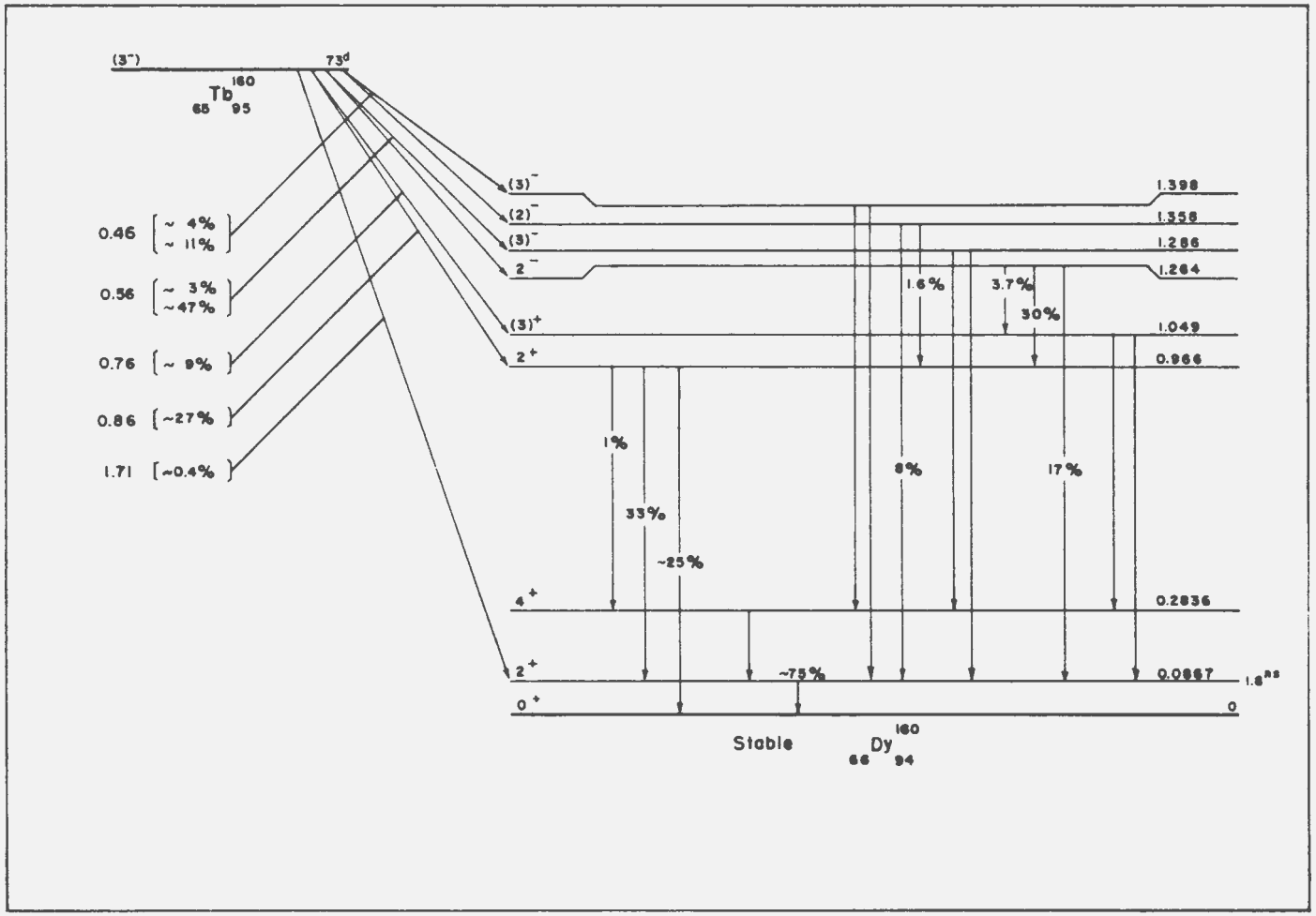

Fig. 19. Decay scheme of Tb^{160}.

$$N_c(87) = N_1(\beta)\, f(345)[1 + \alpha(87)]^{-1}\, \alpha_K(87)\, (\Omega_2) \cdot \epsilon_2(87)\, C(\beta\text{-}87) \quad , \tag{37}$$

where f(345) was estimated to be 0.741 ± 0.027 from the decay scheme branching ratios and the constructed beta spectrum. The C(β-87) factor was assumed to be unity because the angular correlation effects are expected to be small in this case. Any errors introduced by this assumption are expected to be less than 0.2%.

The internal conversion lines of the 87-kev transition are shown in Fig. 20. From these data, the α_K/α ratio was determined to be 0.341 ± 0.011. A corresponding value of 0.281 ± 0.041 was calculated from the data of Grigor'ev *et al.* (73). The value of $(7.38 \pm 0.13) \times 10^{-4}$ 4π steradians given in Appendix A was used for $(\Omega_2)_A$. The area to peak ratio for the 87-kev transition was also determined from the data presented in Fig. 20 and is listed in Table IX. with the remaining quantities used in calculating $\alpha_K(87)$.

The value of $\alpha_K(87)$ determined in this investigation is given in Table X. It is 30% below the theoretical value of Rose (27) and is little more than half the value of Bernstein (26).

The shortcoming of the electron-electron coincidence method for determining large values of α_K which was mentioned

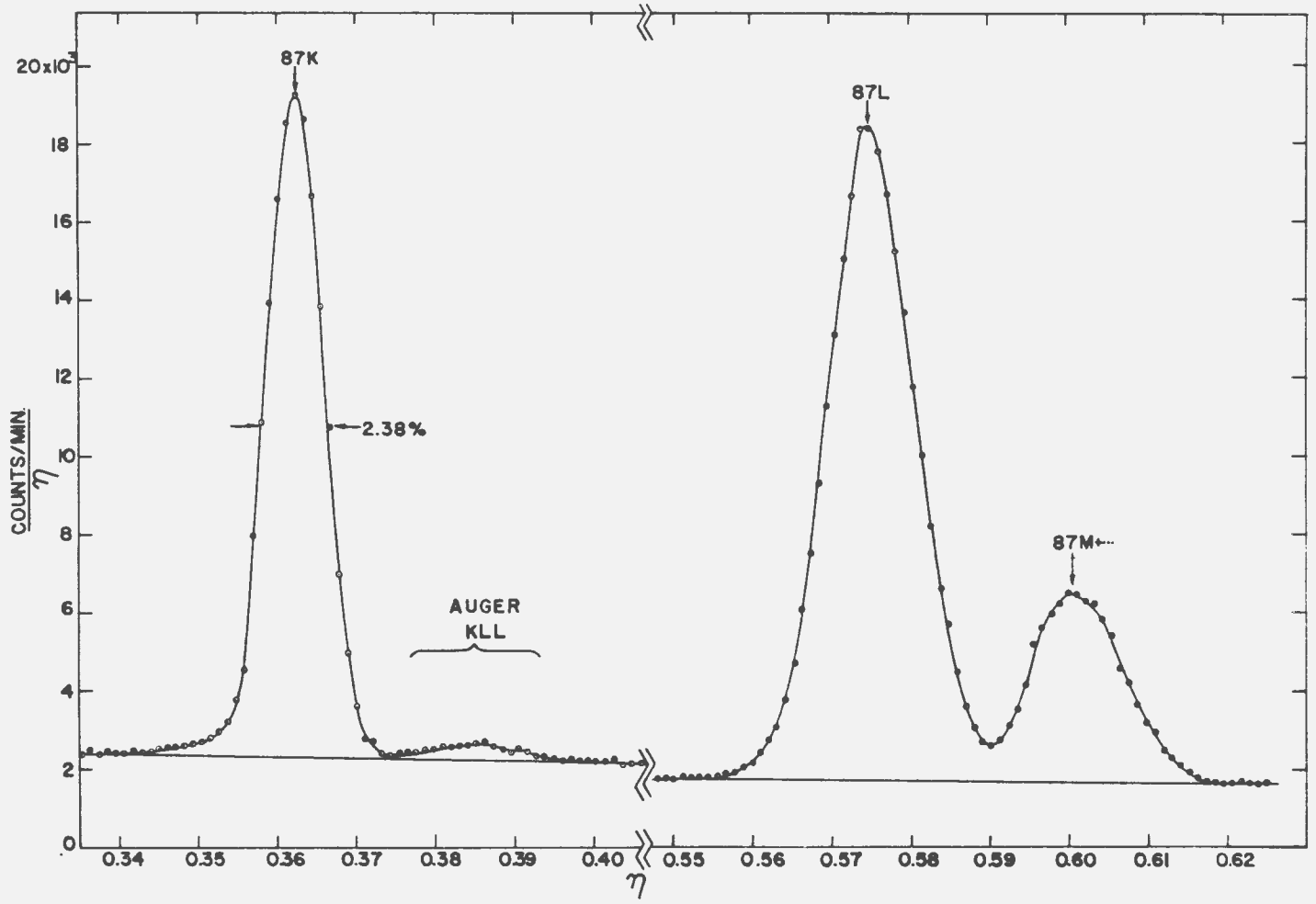

Fig. 20. Internal conversion-electron spectrum of the 87-kev transition in Dy^{160}.

Table IX. Quantities used in the determination of $\alpha_K(87)$

Beta energy	$(N_c/N_1)\times10^4$	(Area/Peak)	ϵ_2	$\frac{\alpha_K(87)}{[1 + \alpha(87)]}$
345	56.6 ± 0.6	0.0242 ±0.0007	0.98 ±0.01	0.256 ±0.013

Table X. α_K of the 86.7-kev transition in Dy^{160}

	$\alpha_K(87)$
Theory (27)	1.50 ± 0.05
Present work	$1.03\ ^{+\ 0.26}_{-\ 0.19}$
Subba Rao (25)	1.75[a] ± 0.20
Bernstein (26)	1.95[b] ± 0.20

[a]An average value based on 4 investigations.

[b]Calculated from $\alpha(87) = 6.02 \pm 0.6$.

in Appendix A is demonstrated in this experiment by the manner in which the 5% error on the $\alpha_K(87)/[1 + \alpha(87)]$ ratio gives a 20% error for $\alpha_K(87)$. Similarly, a 10% increase in this ratio, which is the quantity actually obtained from the

coincidence measurements, increases $\alpha_K(87)$ by 60%. Since the systematic errors introduced into this measurement by the branching ratios of the decay scheme are large, it is difficult to say that the discrepancy with theory is real. This measurement is not in agreement, however, with the value given by Bernstein (26) nor with the higher trend for the measured $\alpha_K(E2)$ values in this region of the deformed nuclei (25,26).